การจำลองคุณลักษณะการเบรกดาวน์ของลูกถ้วยแขวนภายใต้แรงดันอิมพัลส์ฟ้าผ่า

นายคำพะสิด อินทุลาด

วิทยานิพนธ์นี้เป็นส่วนหนึ่งของการศึกษาตามหลักสูตรปริญญาวิศวกรรมศาสตรมหาบัณฑิต
สาขาวิชาวิศวกรรมไฟฟ้า ภาควิชาวิศวกรรมไฟฟ้า
คณะวิศวกรรมศาสตร์ จุฬาลงกรณ์มหาวิทยาลัย
ปีการศึกษา 2557

A SIMULATION OF BREAKDOWN CHARACTERISTICS OF SUSPENSION INSULATORS UNDER LIGHTNING IMPULSE VOLTAGES

Mr. Khamphasith Inthoulath

A Thesis Submitted in Partial Fulfillment of the Requirements
for the Degree of Master of Engineering Program in Electrical Engineering
Department of Electrical Engineering
Faculty of Engineering
Chulalongkorn University
Academic Year 2014

Thesis Title	A SIMULATION OF BREAKDOWN CHARACTERISTICS OF SUSPENSION INSULATORS UNDER LIGHTNING IMPULSE VOLTAGES
By	Mr. Khamphasith Inthoulath
Field of Study	Electrical Engineering
Thesis Advisor	Channarong Banmonkol, Ph.D.

Accepted by the Faculty of Engineering, Chulalongkorn University in Partial Fulfillment of the Requirements for the Master's Degree

.....Dean of the Faculty of Engineering

(Professor Bundhit Eua-arporn, Ph.D.)

THESIS COMMITTEE

.....Chairman

(Assistant Professor Komson Petcharaks, Ph.D.)

.....Thesis Advisor

(Channarong Banmonkol, Ph.D.)

.....External Examiner

(Nutthaphong Tanthanuch, Ph.D.)

คำพะสิด อินทุลาด : การจำลองคุณลักษณะการเบรกดาวน์ของลูกถ้วยแขวนภายใต้แรงดันอิมพัลส์ฟ้าผ่า (A SIMULATION OF BREAKDOWN CHARACTERISTICS OF SUSPENSION INSULATORS UNDER LIGHTNING IMPULSE VOLTAGES) อ.ที่ปรึกษาวิทยานิพนธ์หลัก: ดร.ชาญณรงค์ บาลมงคล, 81 หน้า.

วิทยานิพนธ์ฉบับนี้นำเสนอการจำลองการวาบไฟของพวงลูกถ้วยแขวนจำนวน 1-4 ลูก เนื่องจากแรงดันอิมพัลส์ฟ้าผ่า ด้วยวิธีการอินเกรตและวิธีการเคลื่อนที่ของลีดเดอร์ โดยการจำลองหาลักษณะสมบัติแรงดัน-เวลาของการวาบไฟของพวงลูกถ้วยแขวน เปรียบเทียบกับผลการทดลองในห้องปฏิบัติการ พบว่าการใช้วิธีการเคลื่อนที่ของลีดเดอร์ด้วยพารามิเตอร์ที่นำเสนอสามารถจำลองลักษณะสมบัติแรงดัน-เวลาของการวาบไฟของพวงลูกถ้วยได้ใกล้เคียงกับผลที่ได้จากการทดลองทั้งในกรณีแรงดันอิมพัลส์มาตรฐานรูปคลื่น 1.2/50 μs และแรงดันอิมพัลส์รูปคลื่น 4.8/54.8 μs ทั้งขั้วบวกและลบ นอกจากนี้แบบจำลองที่นำเสนอยังสามารถนำไปใช้ในการประเมินค่าแรงดันวาบไฟวิกฤตของพวงลูกถ้วยแขวนได้อีกด้วย.

ภาควิชา วิศวกรรมไฟฟ้า ลายมือชื่อนิสิต .....

สาขาวิชา วิศวกรรมไฟฟ้า ลายมือชื่อ อ.ที่ปรึกษาหลัก .....

ปีการศึกษา 2557

5570533521 : MAJOR ELECTRICAL ENGINEERING

KEYWORDS: ATP/EMTP / ATPDRAW / LEADER PROGRESSION MODEL (LPM) / LIGHTNING IMPULSE VOLTAGES / SUSPENSION INSULATOR STRING / ANSI CLASS / CRITICAL FLASHOVER VOLTAGES (CFO) / INTEGRATION METHOD (IM)

KHAMPHASITH INTHOULATH: A SIMULATION OF BREAKDOWN CHARACTERISTICS OF SUSPENSION INSULATORS UNDER LIGHTNING IMPULSE VOLTAGES. ADVISOR: CHANNARONG BANMONKOL, Ph.D., 81 pp.

This thesis proposed 2 models for simulating flashover of 1-4 disc suspension insulator strings under lightning impulse voltage, based on integration method and leader progression method. The voltage-time characteristics of insulator strings under 1.2/50 μs standard impulse voltage and 4.8/54.8 μs non-standard impulse voltage of both positive and negative polarities are simulated and compared with laboratory measurements. It is found that the model based on leader progression method with the proposed parameters can provide good results. The proposed model can also be applied to predict the critical flashover voltage of insulator strings with good accuracy.

Department: Electrical Engineering Student's Signature .....
Field of Study: Electrical Engineering Advisor's Signature .....
Academic Year: 2014

ACKNOWLEDGEMENTS

This thesis could not be completed without the kind support and suggestion from many people and organization. First and foremost, I would like to express my sincere thanks to my thesis advisor, Dr. Channarong Banmongkol, who gave good advice and be guidance of this thesis since start until successful. His trust and support me inspired me in the most important moments of making right direction and I am glad to work under his supervision.

I would like to special thank for all of staff, Mr. Thavorn Euady and Mr. Kiangkrai Othanu and friends at high voltage laboratory in department of Electrical Engineering, faculty of Engineering, Chulalongkorn University, for their helpful in providing facilities, theories, material and suggestion for my thesis experiment .

Furthermore, I am also very gratefully acknowledge the JICA project for the financial support during my study at Chulalongkorn University in Thailand under the AUN/SEED-Net scholarship.

Finally, my graduation would not be achieved without my best wish form my mother, who help me everything and always give me greatest love. And the last gratefully special thanks to my friends for their help and encouragement.

CONTENTS

Page

THAI ABSTRACT iv

ENGLISH ABSTRACT v

ACKNOWLEDGEMENTS vi

CONTENTS vii

LIST OF TABLES xi

LIST OF FIGURES xii

CHAPTER 1 THESIS OVERVIEW 1

1.1. Introduction 1

1.2. Motivation of the thesis 2

1.3. Objective of the thesis 3

1.4. Scope of the thesis 3

1.5. Process and method of the thesis 3

1.6. Expectation and benefit from the thesis 4

1.7. Books, research papers and thesis involved 4

1.8. Outline of the thesis 4

CHAPTER 2 THEORY 6

2.1. Introduction 6

2.2. Fundamental in the electrical breakdown processes of gases 6

2.3. Ionization processes 7

2.3.1. Ionization by collision 8

2.3.2. Photo-ionization 8

2.4. Townsend breakdown process 8

Page

2.5. Streamer breakdown process....10
2.6. Surge breakdown time lags....11
2.6.1. Breakdown under impulse voltages....13
2.6.2. Volt-time characteristics....15
2.7. Experimental studies of the time lags....17
2.8. Insulators....17
2.8.1. Properties of insulations....17
2.8.2. Flashover and puncture of insulator....19
2.8.3. Characteristic of the insulators for test and simulation....20
CHAPTER 3 TEST PROCEDURE AND EXPERIMENTAL RESULTS....23
3.1. Experimental method....23
3.2. Experimental circuit....23
3.3. Test objects....24
3.3.1. For ANSI class 52-1 insulator....28
3.3.2. For ANSI class 52-1 insulator....29
3.3.3. For ANSI class 52-1 insulator....30
3.4. Collection data....31
3.4.1. Critical flashover voltages (CFO)....31
3.4.2. Volt-time characteristics....32
3.4.2.1 ANSI class 52-1 insulator string....32
3.4.2.2 ANSI class 52-2 insulator string....33
3.4.2.3 ANSI class 52-4 insulator string....34
3.5. Establishing the volt-time characteristics form testing....35

Page

3.5.1. Under standard lightning impulse voltages 36
3.5.1.1 3-disc ANSI class 52-2 insulator string 36
3.5.1.2 4-disc ANSI class 52-2 insulator string 36
3.5.2. Under non-standard lightning impulse voltages 37
3.5.2.1 3-disc ANSI class 52-2 insulator string 37
3.5.2.2 4-disc ANSI class 52-2 insulator string 37
CHAPTER 4 COMPUTER SIMULATION METHOD 38
4.1. ATP/EMTP 38
4.1.1. ATPDraw 39
4.1.2. TACS 39
4.1.3. MODELS 39
4.2. Model with ATPDraw 40
4.3. Simulating of the insulator strings 43
4.3.1. Integration method (IM) 43
4.3.2. Leader progression model (LPM) 47
4.4. IM & LPM model with ATPDraw 51
4.4.1. Integration method with ATPDraw 53
4.4.2. Leader progression model with ATPDraw 54
CHAPTER 5 SIMULATION RESULTS AND ANALYSIS 57
5.1. Results and comparisons of volt-time characteristics 57
5.1.1. Case of standard lightning impulse (1.2/50 μs) 57
5.1.1.1 ANSI class 52-1 insulators string 57
5.1.1.2 ANSI class 52-2 insulators string 61

Page

5.1.1.3 ANSI class 52-4 insulators string 65
5.1.2. Case of non-standard lightning impulse (4.8/54.8 μs) 66
5.2. Calculation of the percent errors 68
5.3. Determine critical flashover voltages (CFO) 70
CHAPTER 6 CONCLUSIONS AND SUGGESTIONS 75
6.1. Conclusions 75
6.2. Suggestions 76
REFERENCES 77
APPENDIX 80
VITA 81

LIST OF TABLES

Page

Table 3-1 Critical flashover voltages 31

Table 4-1 The constant values of *K* and E_0 proposed in ref. [4].....50

Table 4-2 The constant values of *K* and E_0 proposed in ref. [5] 50

Table 4-3 The constant values of *K* and E_0 for model.....51

Table 5-1 The maximum percent errors for standard lightning impulse.....69

Table 5-2 The maximum percent errors for non-standard lightning impulse 70

Table 5-3 Gap lengths of ANSI 52-4 with arcing horn rod-rod gap 71

Table 5-4 The constant values *K* and E_0 for ANSI Class 52-4 insulator string with arcing horns.....72

Table 5-5 The percent errors for CFOs of 1-4 disc insulator strings without arcing horn 73

Table 5-6 The percent errors for CFOs of 4-7 disc insulator strings with arcing horns.....74

LIST OF FIGURES

Page

Figure 2.1 Visualization of a Townsend avalanche 9

Figure 2.2 Effect of space charge produced by an avalanche on the applied electric field 10

Figure 2.3 Cathode direct streamer 11

Figure 2.4 Step voltage time lag 12

Figure 2.5 General wave shape of lightning impulse (LI) voltage 14

Figure 2.6 Breakdown under impulse voltage 15

Figure 2.7 Breakdown volt-time characteristic 16

Figure 2.8 Volt-time characteristic of uniform and non-uniform field gap 16

Figure 2.9 The leakage distance 18

Figure 2.10 Dry arcing distances of 1 disc and 4 discs insulators strings 19

Figure 2.11 Volt-time characteristics of an insulator 20

Figure 2.12 Main dimension of a string of suspension insulators 22

Figure 3.1 Equivalent diagram of experimental circuit 24

Figure 3.2 Dimension of ANSI class 52-1 insulator 25

Figure 3.3 Dimension of ANSI class 52-2 insulator 25

Figure 3.4 Dimension of ANSI class 52-4 insulator 25

Figure 3.5 Dry arcing distances of ANSI class 52-1 insulator string (*a*) 1 disc, (*b*) 2 discs and (*c*) 3 discs 26

Figure 3.6 Dry arcing distances of ANSI class 52-2 insulator string (*a*) 1 disc, (*b*) 2 discs, (*c*) 3 discs and (*d*) 4 discs 27

Figure 3.7 Dry arcing distances of ANSI class 52-4 insulator 1 disc 27

Figure 3.8 Dry arcing distance as a function of number and height of disc for ANSI class 52-1 insulator....28

Figure 3.9 Dry arcing distance as a function of number and height of disc for ANSI class 52-2 insulator....29

Figure 3.10 Dry arcing distance as a function of number and height of disc for ANSI class 52-4 insulator....30

Figure 3.11 Volt-time curves of 1-disc ANSI class 52-1 insulator....32

Figure 3.12 Volt-time curves of 2-disc ANSI class 52-1 insulator string....32

Figure 3.13 V'olt-time curves of 3-disc ANSI class 52-1 insulator string....33

Figure 3.15 Volt-time curves of 2-disc ANSI class 52-2 insulator string....34

Figure 3.17 An example of distribution of chopping time for each applied voltage level....35

Figure 3.19 Volt-time curve of 4-disc ANSI class 52-2 insulator string....36

Figure 3.20 Volt-time curve of 3-disc ANSI class 52-2 insulator string....37

Figure 3.21 Volt-time curve of 4-disc ANSI class 52-2 insulator string....37

Figure 4.1 Simulation circuit....40

Figure 4.2 The comparison of lightning impulse between experiment and simulation....41

Figure 4.3 Front wave shape of simulated lightning impulse voltages....42

Figure 4.4 Tail wave shape of simulated lightning impulse voltages....42

Figure 4.5 Integration method....43

Figure 4.6 *DE* equation for (*a*) Positive polarity and (*b*) Negative polarity....45

Figure 4.7 Integration method's breakdown flowchart....46

Figure 4.8 The development of leader and the breakdown process....48

Figure 4.10 IM & LPM model with ATPDraw....51

Figure 4.11 Input data for Sources 52

Figure 4.12 Input data for IM & LPM MODELS 52

Figure 4.13 Case of breakdown in with integration method in ATPDraw 53

Figure 4.14 Case of no breakdown in with integration method in ATPDraw 54

Figure 4.15 Case of breakdown in with LPM in ATPDraw 55

Figure 4.16 Case of no breakdown in with LPM in ATPDraw 55

Figure 4.17 Volt-time characteristic from the IM & LPM model 56

Figure 5.2 The comparison between volt-time characteristics which obtained from experiment and simulation of 2-disc ANSI class 52-1 insulator string under standard lightning impulse voltages of (*a*) Positive polarity and (*b*) Negative polarity 59

Figure 5.3 The comparison between volt-time characteristics which obtained from experiment and simulation of 3-disc ANSI class 52-1 insulator string under standard lightning impulse voltages of (*a*) Positive polarity and (*b*) Negative polarity 60

Figure 5.4 The comparison between volt-time characteristics which obtained from experiment and simulation of 1-disc ANSI class 52-2 insulator under standard lightning impulse voltages of (*a*) Positive polarity and (*b*) Negative polarity 61

Figure 5.5 The comparison between volt-time characteristics which obtained from experiment and simulation of 2-disc ANSI class 52-2 insulator string under standard lightning impulse voltages of (*a*) Positive polarity and (*b*) Negative polarity 62

Figure 5.6 The comparison between volt-time characteristics which obtained from experiment and simulation of 3-disc ANSI class 52-2 insulator string under standard lightning impulse voltages of (*a*) Positive polarity and (*b*) Negative polarity 63

Figure 5.7 The comparison between volt-time characteristics which obtained from experiment and simulation of 4-disc ANSI class 52-2 insulator string under standard lightning impulse voltages of (*a*) Positive polarity and (*b*) Negative polarity 64

Figure 5.8 The comparison between volt-time characteristics which obtained from experiment and simulation of 1-disc ANSI class 52-4 insulator under standard lightning impulse voltages (*a*) Positive polarity and (*b*) Negative polarity 65

Figure 5.10 The comparison between volt-time characteristics which obtained from experiment and simulation of 4-disc ANSI class 52-2 insulator string under non-standard lightning impulse voltages of (*a*) Positive polarity and (*b*) Negative polarity 67

Figure 5.11 Breakdown probability distribution 70

CHAPTER 1

THESIS OVERVIEW

1.1. Introduction

Insulators are an essential apparatus in electrical power transmission and distribution systems. They are always subjected to 1) external overvoltages from atmospheric discharges or lightning and 2) internal overvoltages from switching or fault initiation etc. For tropical countries, lightning surge is a main problem which leads to faults in the power systems. Because lightning overvoltages can cause high dielectric stress, which may be higher than the impulse strength of the insulation. It affects directly to the insulators to cause a damage and lead to breakdown in the power systems. The study about the behaviors and the characteristics under the lightning overvoltages are very important in the power protection system including insulation co-ordination systems [1, 2]. The whole for limiting and reducing the damages which will occur in the insulators as well as the electrical power systems.

Several previous researches have been done to understand the fundamental characteristics of the electrical discharge and breakdown [3-10]. They defined the formulas which use to calculate these electrical behaviors. Then, several methods have been proposed. Among them, the integration method and the differential equation i.e. leader progression model are widely used. Both methods were used to calculate and simulate several of gap i.e. a small air gap until very large air gap. Almost all of the previous studied, they studied breakdown characteristics in various air gaps i.e. arcing horn rod-rod gap, arcing horn sphere-sphere gap, electrode rod-plane gap etc., to calculate the breakdown voltages and times to breakdown. When bring these data plot in a graph, while X-axis is times to breakdown and Y-axis is breakdown voltages, after that draw a curve along through each point of them. This curve was called as volt-time characteristic or volt-time curve. Therefore, electrical breakdown characteristic of an insulator string with the different number of discs under the

different applied lightning impulse voltages have great significance for the design of the overhead transmission line systems.

1.2. Motivation of the thesis

The magnitude of the lightning overvoltages remains essentially independent of the system's design. The well-known of the volt-time characteristics of the insulators are significance for the insulations co-ordination in the electrical power systems. The volt-time characteristic illustrate the relation between the breakdown voltages and the times which lead to breakdown. It can be tested and established in high voltage laboratory by stressing the lightning impulses to the insulators. But it is difficult and time consumption i.e., to set the apparatus, the measurements instruments etc. An alternative method is using the computer software to help establishing the volt-time characteristics. The popular software which be used to simulate is Alternative Transients Program/Electromagnetic Transients Program (ATP/EMTP) [11-13]. The leader progression model have been selected to simulate in ATP/EMTP, this method has been proposed by CIGRE [3]. The leader progression model is more flexible than the integration method, this method can offer the breakdown volt-time characteristics of any impulse wave shape with positive and negative polarities, any gap configurations, any gap lengths (up to 7 m) [4], and this method was modified in many versions [6, 7].

In this study collected data from previous studies [14, 15] and tested the air breakdown voltages experimentally in high voltage laboratory at Chulalongkorn University. The insulator strings with various number of discs were used to test for collection the experimental results i.e. volt-time characteristics and critical flashover voltages. The insulator stings which be used to test and simulate in this study consist of ANSI class 52-1, 52-2 and 52-4. The experimental results as mentioned earlier are conducted at normal temperature and pressure, as well as the influence of the humidity on breakdown characteristic test has been also considered in this thesis.

The aim of this thesis is to create a model to simulate the breakdown characteristics. This model has been carried out in the ATPDraw which a graphic

software include ATP/EMTP, and base on leader progression model (LPM). Finally, the experimental results have been compared with the simulation results and their errors have been proposed and analyzed.

1.3. Objective of the thesis

1. To perform the practical experiment of air breakdown voltages in high voltage laboratory and study the important theories of understanding the performance characteristics of the air breakdown voltages.
2. To find the air breakdown voltages of the insulator strings and their characteristics which plot versus time to breakdown.
3. To understand the breakdown simulation program i.e. ATP/EMTP and ATPDraw.
4. To create the breakdown model which carry out in the ATPDraw by using leader progression model (LPM) and establish the volt-time characteristics.
5. To compare between the volt-time characteristics which obtained from the model and the experimental results.

1.4. Scope of the thesis

1. Develop a breakdown simulation in computer software by using the ATP/EMTP.
2. Establish the volt-time characteristics of the suspension insulator strings.
3. Test and simulate under lightning impulse only.

1.5. Process and method of the thesis

1. Determine the scope of the thesis purpose.
2. Study the research papers and the thesis involved.
3. Study the fundamental theory and the calculation method of the breakdown simulations.

4. Collect the important data from the previous researches and laboratory experiment methods.
5. Use the 3rd and 4th processes for developing a breakdown simulation.
6. Collect all the information which received and evaluate the results.
7. Write the thesis.

1.6. Expectation and benefit from the thesis

1. Can establish the volt-time characteristics nearby with the original.
2. To be helpful to establish volt-time characteristics from the breakdown simulation. Hence, be unnecessary to test in laboratory.

1.7. Books, research papers and thesis involved

In this thesis studied on the characteristics of air breakdown voltages. This study offer a part of the co-ordination insulation systems[1, 2]. Some experimental obtained from the practical test in high voltage laboratory which followed ref. [16, 17], and received from the previous research [14, 15]. To create the breakdown model with ATPDraw [11-13] by using the leader progression model. Ref. [3, 4] provided the guideline for this model, and this model was used and modified in many researches e.g. ref. [5] used this model to determine the volt-time characteristics and the critical flashover voltages (CFO), ref. [7] was modified this model to calculate leader development characteristics for long gaps of several meters, ref. [6] compared the various modified methods which base on this method and other methods. Also, still have the fundamental theories form books which discussed about breakdown in gases [18-25] and discussed about the insulators [26, 27]. And the thesis references which guide to write this thesis [15, 28].

1.8. Outline of the thesis

The thesis is consist of six chapters in which each chapter has its own way of describing and analyzing the fundamentals of the work which followed the theories, experimental setup and simulation results.

CHAPTER 1: This chapter deals with the thesis overview such as: the basic introduction, motivation, objective, scope, process, method, expectation and benefit of the thesis.

CHAPTER 2: In this chapter discussed about the theories of breakdown. It also covers the fundamental definition of air breakdown voltages for example breakdown mechanisms, breakdown time lags, breakdown under lightning impulse voltages, breakdown volt-time characteristics etc. And discussed about the insulator strings and their dimensions.

CHAPTER 3: This chapter discussed about the experimental method, collection data, and equivalent diagram of experimental circuit. Determining the chopping times or the times lead to breakdown. And shown these data.

CHAPTER 4: In this chapter deals with the function and benefits of a computer software to use to a model to simulate the volt-time characteristics i.e. ATP/EMTP as well as ATPDraw, shown the basic the simulation circuit and the method to use to create the IM & LPM model. How to determine the value which use in this model

CHAPTER 5: In this chapter shown the results of comparison between experimental and the simulation and analysis their errors.

CHAPTER 6: This chapter is final chapter which deals with the conclusion the suggestion of this thesis.

CHAPTER 2

THEORY

2.1. Introduction

The main characteristic of insulating materials are preventive discharge which may occur during the application of stress. However, these material cannot resist infinite amounts of voltages stresses. An insulating material is also called as a dielectric which mean a material that resists the flow of electric charge. These materials are used in electrical apparatus as insulation. Their function is to support or separate electrical conductors with without allowing current through themselves. Breakdown voltage is well-known as a characteristic of an insulator which is the minimum voltage that causes a portion of an insulator to become electrically conductive and collapses. Breakdown voltage is also called the striking voltage [18]. The breakdown voltage of the insulation are grouped broadly into three groups like: (i) Self-restoring i.e. gases which no change produced by the application of stress or by breakdown voltage or by discharge, hence, can test the simple many times. (ii) Non-self-restoring i.e. liquids which are affected by discharge only, these materials can be used until discharge occurs. And (iii) Affected by applied stress i.e. solids which has the insulation experiences ageing and in testing of these materials should ponder to their dielectric strength. In this thesis will talk about the breakdown in gases only. To obtain a better understanding of the fundamental processes of dielectric i.e. gas-breakdown are summarized and the equations are given. For extensive principles of the breakdown of gases see Meek and Craggs [18], Townsend [19] and the other books which discussed about this topic namely “High Voltage Engineering” [20-25].

2.2. Fundamental in the electrical breakdown processes of gases

The simplest and the most commonly use dielectrics are gases. The majority of the electrical apparatus use air as the insulating medium. Air at atmospheric pressure is the most common gaseous insulation. The breakdown in air is important to the

design engineer of power transmission lines and power apparatus. When a voltage is applied to the apparatus, there are numerous phenomenon occur in gaseous insulation. In normal condition, these material offer a very high resistance to a voltage and its currents cannot flow between the electrodes through the insulation. However, when the applied voltage and the current grow very shapely, they cannot withstand an infinitely high voltage, and the breakdown phenomenon occurs. The voltage breakdown is the maximum voltage which applied to the insulation at the moment of breakdown. To understand the breakdown phenomenon in gases, the electrical properties of gases should be studied. The processes by which high currents are produced in gases are essential. The electrical discharge in gases are two type [20]:

(*a*) Non-sustaining discharges.

(*b*) Self-sustaining discharges.

The transition of a non-sustaining discharge into a self-sustaining discharge is called the breakdown in gases. The rising of high voltage in a breakdown is due to the process known as ionization, in which electron and ions are produced from neutral atoms and molecules, and move to the anode and cathode respectively, leads to high voltage. At the present, the breakdown phenomena can explain in two types of theories or mechanisms:

(*a*) Townsend theory.

(*b*) Streamer theory.

The well-known, the two of theories explained the mechanism for breakdown process under different condition. The various physical condition of gases, there are temperature, pressure, electrode configuration, electric field, nature of electrode surfaces and the availability of initial conducting particles as known to govern the ionization processes.

2.3. Ionization processes

As mentioned above, in normal condition, a gas has perfected insulators. On other hand, during a high voltage apply to between two electrodes in a gaseous medium, the gas becomes a conductor and occurs the electrical breakdown. The

breakdown of gas is brought about by various processes of ionization, e.g., ionization by collision, photo-ionization, and the secondary ionization processes.

2.3.1. Ionization by collision

If the kinetic energy are gained by an accelerated electron is larger than the ionization energy threshold of the gas molecule or atom, this ionization may take place in which an electron and a positive ion are formed. It mean that number of ionizing collision per electron travel a unit length in the direction of the electric field is termed "Townsend's first ionization coefficient (α)". This process can be represented as:

$$A + e^- \rightarrow A^+ + 2e^- \tag{2.1}$$

Where A is the atom, A^+ is the positive ion and e^- is the electron

A few electrons are produced at the cathode, ionize neutral gas particle produce positive ions and additional electrons. Then, this additional electron make ionizing collision by themselves and thus the process repeats itself.

2.3.2. Photo-ionization

Photo-ionization occurs when the number of radiation energy absorbed by a gas molecule or atom exceeds its ionization potential. Thereby creating an electron and positive ion. This process can be expressed as:

$$A + h\nu \rightarrow A^+ + e^- \tag{2.2}$$

This process occurs when

$$\lambda \leq c \times \frac{h}{V_i} \tag{2.3}$$

Where, *h* is the Planck's constant, *c* is light velocity, λ is the wavelength of the incident radiation and V_i is the ionization energy of the atom.

2.4. Townsend breakdown process

One of the process which considered a description of the fundamentals of steady-state gas discharge was put forth by Townsend [19], and the well-known form

of breakdown bears his name. Townsend breakdown mechanism is based on the generation of successive secondary avalanches to produce breakdown, a voltage is applied across two electrodes of a gas-filled discharge gap. Electron in the gap with a sufficiently high electric field in a gaseous medium which can be ionized i.e., air. Following an original ionization event, due to such as ionizing radiation, the positive ion leads towards the cathode, while the free electron lead towards the anode of the device. If the electric field strength is high enough, then it is likely to ionize a gas molecule by simple collision, the free electron gains sufficient energy to liberate a further electron when it next collides with another molecule. The two free electron then drift the anode and gain sufficient energy form electric field to cause impact ionization when the next collision occur; and so on. This is effectively a chain reaction of electron generation and dependent on the free electrons gaining sufficient energy between collisions to sustain the avalanche.

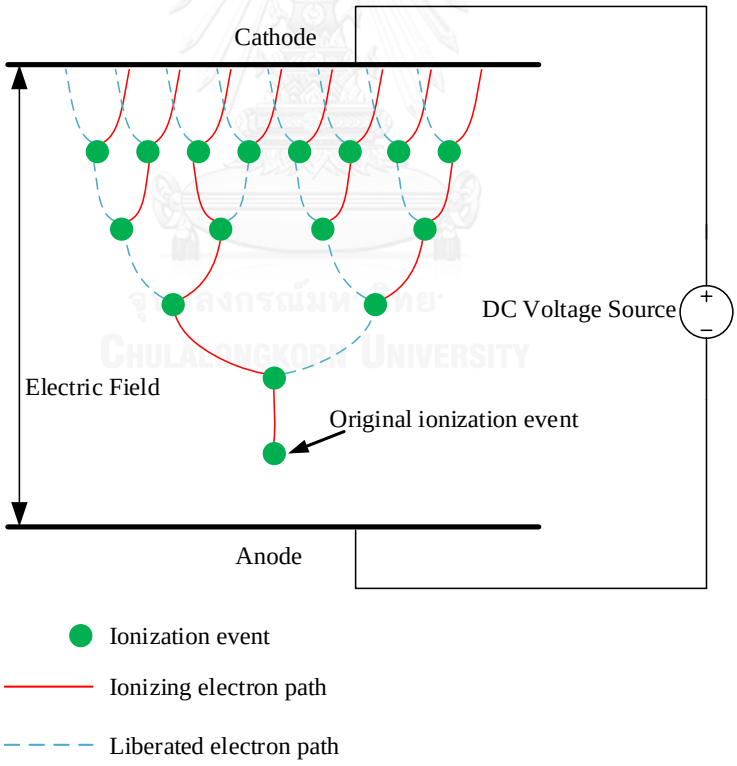

Figure 2.1 Visualization of a Townsend avalanche

2.5. Streamer breakdown process

Townsend theory cannot explain certain events when applied a voltage to breakdown at atmospheric pressure. Firstly, according to this theory, current growth occurs as a result of ionization processes only. But in practice, breakdown voltages were found to depend on the geometry of gap and the gas pressure. Secondly, the breakdown process predicts time lags of the order of 10^{-5} sec., while in the practice the breakdown was observed to occur at very short times of the order of 10^{-8} sec. and while the Townsend estimates a much diffused form of discharge, in the actual practice, discharge were found to be filamentary and irregular. The Townsend mechanism failed to explain all these observed phenomena. Around 1940, Raether and, Meek and Loeb proposed the Streamer theory [20].

The theories predict the development of a spark discharge directly from a single avalanche in which the space charge developed by the avalanche itself is said to transform the avalanche into a plasma streamer.

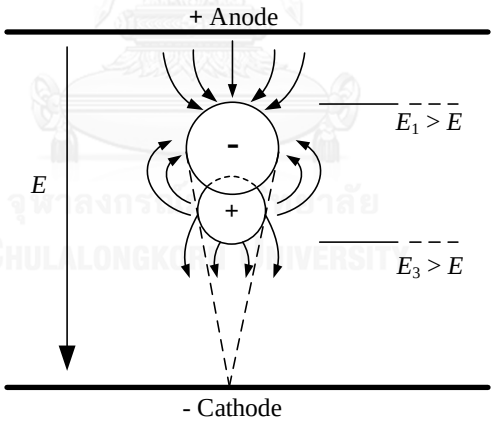

Figure 2.2 Effect of space charge produced by an avalanche on the applied electric field

According to figure 2.2, a single electron start at the cathode by ionization builds up an avalanche that crosses the gap. The electron in the avalanche travel very fast compared with the positive ions. At this time the electron reach to the anode, the positive ions are virtually in their original position and form a positive space charge at the anode. This increasing the field and the secondary avalanches are formed by the

few electrons which produced due to photo-ionization in the space charge area. This occurs first near the anode where the space charge is maximum. Their result in a further increase in the space charge. The process is so fast and the positive space charge extends to the cathode rapidly resulting in the formation of a streamer. The narrow luminous tracking occur while the breakdown at high pressures are called streamer. There are three continual stages in the development of the streamer as shown in figure 2.3, in which (*a*) illustrates the stage when avalanche has crossed the gap, (*b*) illustrates the streamer has crossed half of the gap length and (*c*) illustrates the gap has been bridged by a conducting channel.

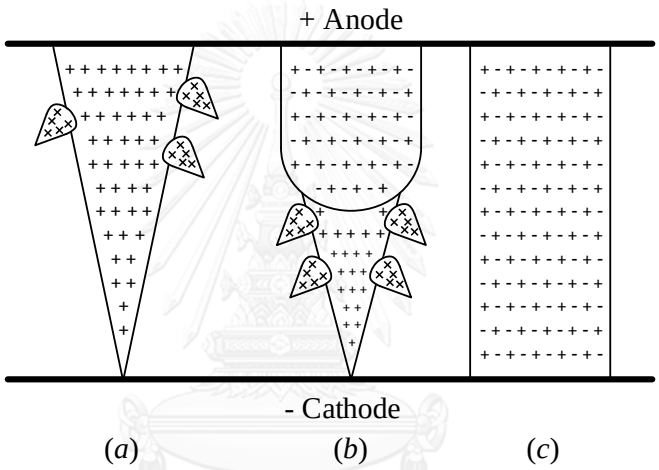

Figure 2.3 Cathode direct streamer

2.6. Surge breakdown time lags

Under a surge voltage and pulse of short duration time, the gap may not breakdown when the peak voltage reaches the lowest breakdown value V_S. V_S is a minimum voltage which can lead to breakdown of the gap after a period of time of voltage applied. The figure 2.4, illustrates the breakdown under a step voltage; V_P is the peak value of a step voltage which applied at time t = 0 to the gap that can occur the breakdown when V_P has been greater than V_S after a period of time.

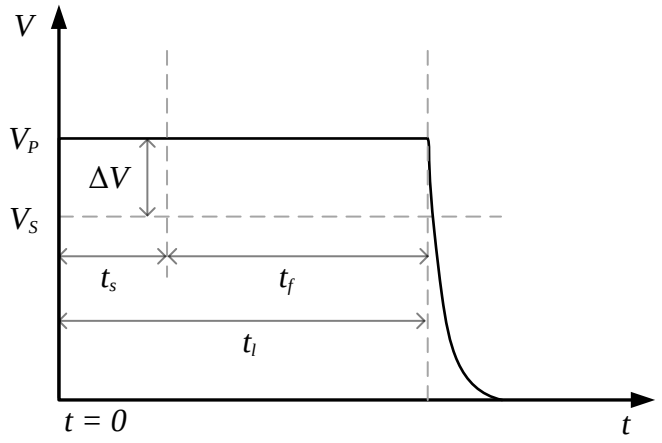

Figure 2.4 Step voltage time lag

Where:

V_S - Minimum static breakdown voltage

V_P - Peak voltage

t_s - Statistical time lag

t_f - Formative time lag

The period of time between the applied voltage to a gap enough to occur breakdown and this period of time was called as the time lag (t_l). This time consists of two component of time [18]: first time is a time which lapses during the application of voltage sufficient until can found a primary electron which strength enough to initiate the discharge, this time is called the statistical time lag (t_s). And the other is a time which required for the ionization processes to sufficiently develop to cause the breakdown of the gap and is known as the formative line lag (t_f).

The statistical time lag (t_s) depends on the number of pre-ionization in the gap, including the length of the gap and the radiation which produce the primary electrons. The electrons appears to initiate the discharge is usually statistically distributed. The statistical time lag can be reduced by the difference in the voltage $\Delta V = V_p - V_S$ and ΔV is called that the overvoltage.

The formative time lag (t_f) depend mainly on the mechanism of breakdown. In case of the secondary electron arise entirely from electron emission at the cathode

by positive ions, the moving time from anode to cathode will be the dominant factor determining the formative time. The formative time lag increase with the increasing of the gap length and the field non-uniformity, but it decreases with the increasing of the overvoltage.

2.6.1. Breakdown under impulse voltages

An impulse voltage is a voltage which unidirectional, this kind of voltage is rapid rising to a maximum value and then decay slowly to zero when compared with its rising. The impulse voltage consist of two kinds [21]:

The first kind is the lightning impulse, it origin form lightning strokes. The amplitude are very high, usually in the order of 1000 kV or more, each stroke bring the travelling waves to transmission line. If its amplitude is too high voltage level, the breakdown has occurred by chopped at the insulation i.e. insulators. Therefore, the traveling waves with steep wave fronts, even steeper wave tails may stress into the insulation e.g., power transformer or other high voltage apparatus severely.

The second kind is caused by rejecting or injecting load in the power systems. The amplitudes of this kind of impulse are always related due to the operating and shape is influenced by the impedance of the systems and by the switching condition too. Normally, their amplitudes are lower than the first kind and their rate of voltage rise is also slower than, but their duration of steady time is longer than the first kind. The wave shape can also very dangerous with the insulation systems because of their duration of steady time.

Both kind of overvoltages became necessary to simulate these transient overvoltages by the various computer software as well as for testing purpose the high voltage apparatus. The various national and international standards give the definition of the impulse voltages as a unidirectional voltage. In the relevant IEC standard 60 [16], are widely accepted. In general, considered as lightning impulses as shown in figure 2.5. The most applications, the front time $T_1 = 1.2\ \mu s$, and the time to half-value $T_2 = 50\ \mu s$. The tolerances of T_1 can be up to $\pm 30\%$ and $\pm 20\%$ for T_2. Then the

lightning impulse voltages are referred to as $T_1 / T_2 = 1.2 / 50\ \mu s$. This shape is the accepted standard lightning impulse voltage today as shown in the figure 2.5.

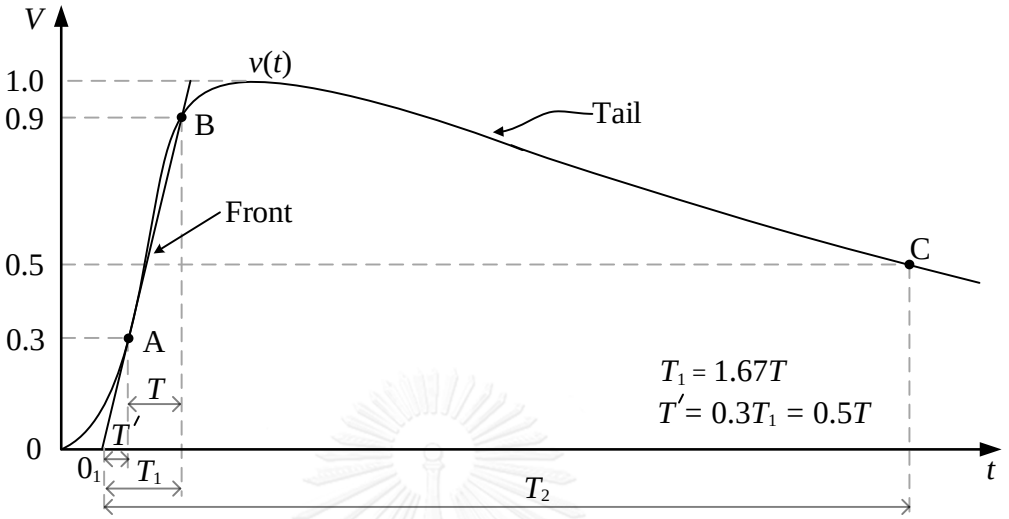

Figure 2.5 General wave shape of lightning impulse (LI) voltage

When apply an impulse voltage with a peak value V_P and let it's higher than V_S in a gap, at the moment $V_P = V_S$ is marked by time t_1 as shown in the figure 2.6. There is a certain of probability to occur the breakdown, but it won't occur immediately because of the time lag as mentioned before. The overvoltage (ΔV) duration have to exceed the time lag (t_f). When gain the amplitude of impulse voltage exceed the static value (V_S) until occur breakdown at this moment is marked by chopping time (t_c). In the practice, the chopping time is not constant value, it depend on the various values as whole mentioned. Therefore, obtain a breakdown probability (*P*) for each number of maximum impulse voltage (V_P) as a function of time ($v(t)$).

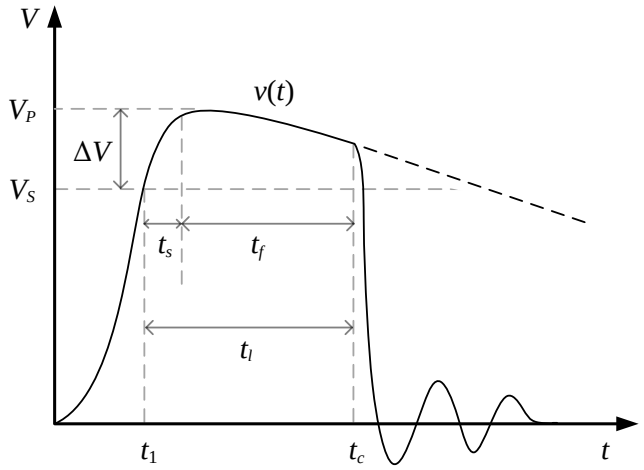

Figure 2.6 Breakdown under impulse voltage

The total of time lag can be expressed by equation below

$$t_l = t_s + t_f \tag{2.4}$$

The maximum of impulse voltage (V_P) must be higher than the statistic breakdown voltage (V_S). The ratio between V_P and V_S (V_P/V_S) is called as impulse ratio and the differential between V_P and V_S ($\Delta V = V_P - V_S$) is called as the overvoltage. They are helpful in the system design and co-ordination insulation.

2.6.2. Volt-time characteristics

When an impulse voltage is high enough to cause the breakdown, the breakdown voltage will receive on each voltage application. If the voltage as function of time ($v(t)$) chopped at the tail wave of impulse, in this case the peak of impulse voltage provide the breakdown voltage. If it chopped at the front wave of impulse, the breakdown voltage is provided by the maximum voltage at the point which chopped. The time lag depend on the breakdown voltages and the field geometry. Therefore, a volt-time characteristic is constructed by the number of breakdown voltage against their time lag. The schematic plot of breakdown voltages (V_b) against chopping times (t_c) was shown in the CHAPTER 3.

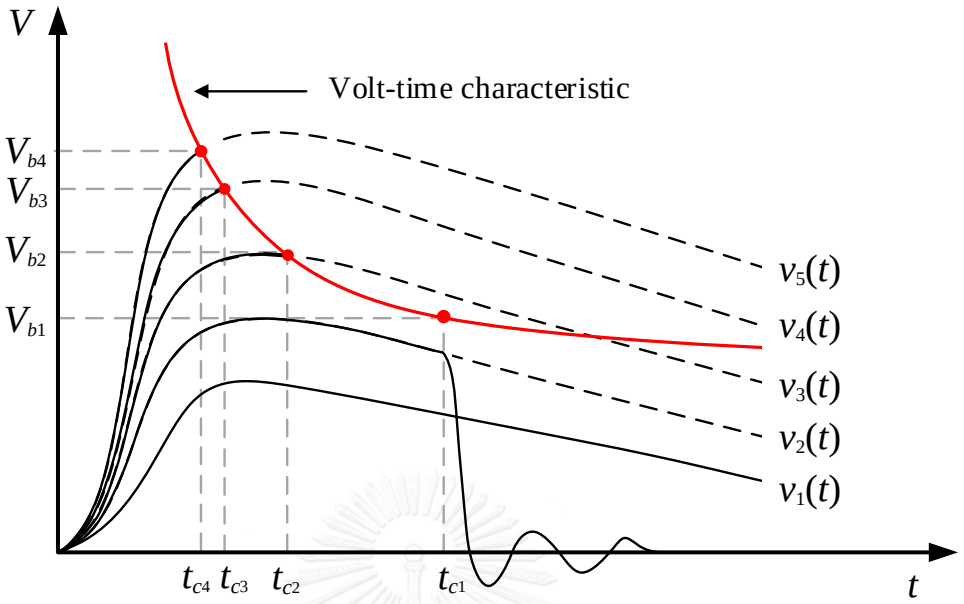

Figure 2.7 Breakdown volt-time characteristic

In quasi-uniform and uniform field gap, the characteristic is usually shapely defined and its curve rises with increasing the rate of rise of the applied voltage. However, in non-uniform field gap, due to larger scatter in the results, the data fall into a dispersion band as shown in the figure 2.8. The chopping time is less sensitive to the rate of voltage rise. Hence, quasi-uniform field gap i.e. sphere-sphere gap have often used as protective device against overvoltages.

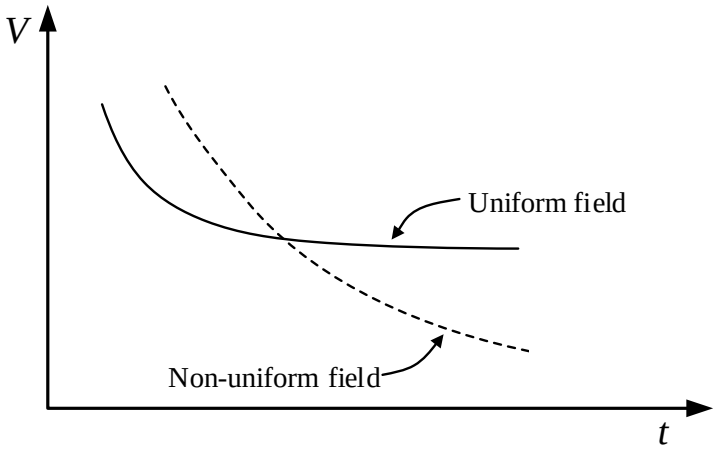

Figure 2.8 Volt-time characteristic of uniform and non-uniform field gap

The volt-time characteristic is an important for co-ordination insulation systems. It provides the basis for the impulse strength of the insulation and for the design of the protective devices against overvoltages.

2.7. Experimental studies of the time lags

There are numerous previous researches have studied about the time lags in the past. The general techniques used either a constant voltage which applied into an irradiated gap and a spark is initiated by sudden illumination of the gap from a nearby spark. In the former case the time lag is measured from the flash until breakdown occurs, while in the latter the time lag is measured between the voltage application and the gap breakdown. The measurement of time lags for given experimental conditions are usually are presented graphically by plotting the average time lags against the breakdown voltages.

2.8. Insulators

The insulators are an electrical device which be used on electricity supply networks to support, separate or contain conductors at high voltage. A special case, the insulators are used in the maintenance service of live apparatus [26]. All of the insulators include dual function like mechanical and electrical. The main function of the insulators separate line conductors and the supports i.e. the tower to provide perfect insulation between the conductors and the supports and to resist the leakage current form the line conductors to earth through the support.

2.8.1. Properties of insulations

To provide necessary insulation, the insulators must have the following properties:

1. The insulators provide the insulation and also provide to support the conductors. Hence, the insulators must mechanically very strong.
2. The insulator must have very high insulation resistance to prevent any leakage current.

3. The insulators must be free from internal impurities such as cracks, holes, laminations etc. These impurities can reduce the permittivity of the insulators.
4. The dielectric strength of the insulators must be very high.
5. The relative permittivity of the insulating material should be very high to provide high dielectric strength.
6. The material of the insulators should be non-porous.
7. The insulators should not affect when the temperature change.
8. Due to very high voltages or overvoltages, there is high chance to occur a flashover or puncture along the insulators to earth. The flashover is a disruptive electrical discharge around or over the surface of the insulators. And the puncher is a breakdown and this breakdown caused an electric arc through the interior the insulator. This is the main cause of insulator failures and collapses. Thus, the ratio of puncture strength must be higher than the flashover voltages. This value can see the manufacturer specifications such as impulse strength, leakage distance, dry arcing distance etc.
9. Leakage distance is the sum of the shortest distance measured along the insulator surfaces between the terminal electrode parts, as arranged for dry flashover test. As figure 2.9, the red line is the leakage distance.

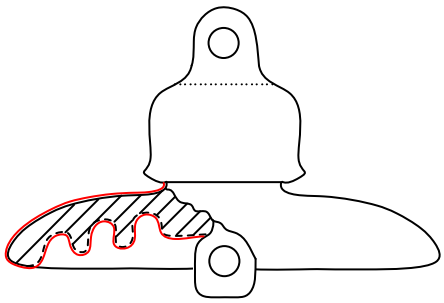

Figure 2.9 The leakage distance

10. Dry arcing distance is the shortest distance through the surrounding medium between terminal electrodes, or the sum of distances between intermediate electrodes, whichever is shortest, with the insulator mounted for dry flashover test. As figure 2.10, the red lines are the dry arcing distances.

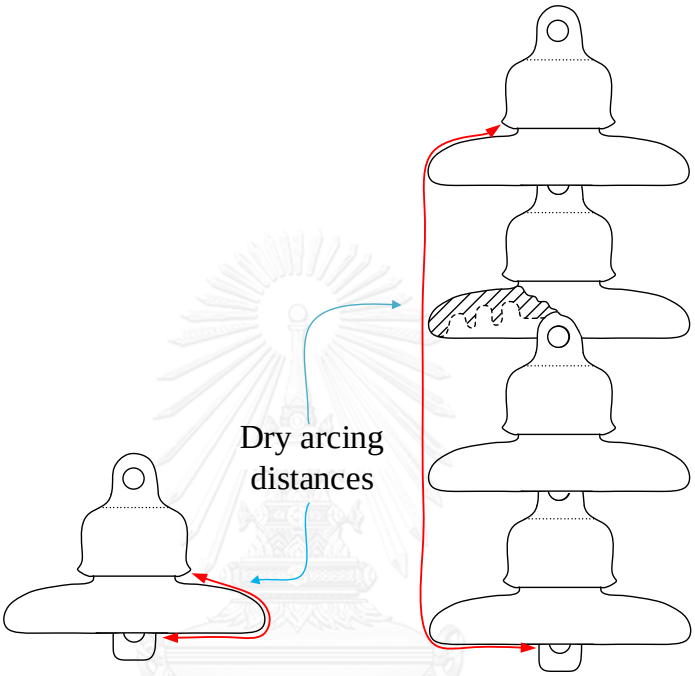

Figure 2.10 Dry arcing distances of 1 disc and 4 discs insulators strings

2.8.2. Flashover and puncture of insulator

When applied an impulse voltage to an insulator until occurs the flashover around an insulator surface, its breakdown volt-time characteristic is the curve A in the figure 2.11, and the breakdown voltage can puncture to interior material of an insulator, a puncture characteristic is the curve B in the same figure. The point S_c is the intersection between curve A and curve B which illustrate the relation between the puncture and flashover of an insulator. It mean that, if a breakdown voltage is higher than the point S_c like the breakdown voltage V_{b2}, the breakdown voltage will puncture to interior material of insulator. Whereas, a breakdown voltage is lower than the point S_c like the breakdown voltage V_{b1}, the breakdown voltage will flashover around insulator surface. The effect of puncture of an insulator mean that the insulator will

be permanently collapse. Hence, designing of the insulator always provide to occur flashover before puncture.

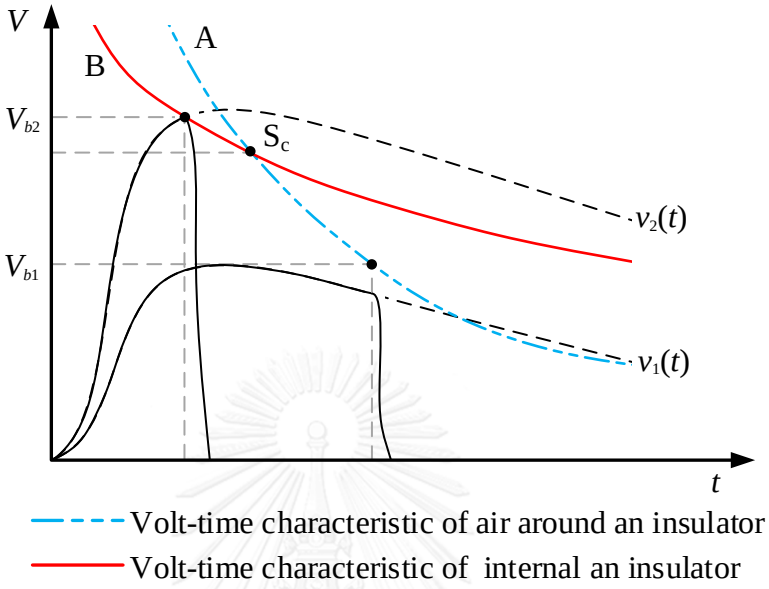

Figure 2.11 Volt-time characteristics of an insulator

2.8.3. Characteristic of the insulators for test and simulation

The insulators which be used to test and simulate in this thesis focus on the porcelain suspension type insulator. Firstly, will talking about the material i.e. porcelain and type of the insulator i.e. suspension type insulator.

The porcelain is the most commonly used as material for the insulators, it is manufactured from the plastic clay which be mixed with silicon and feldspar, if good manufacture (free form cracks, holes, lamination etc.), its dielectric strength is about 60 kV/cm [27].

The suspension insulators are the most popular insulators used for high voltage transmission lines systems. This type consist of number of porcelain discs unit and install as a string. The string comprise of many discs which be connected to another discs in series with the help of metal link, and this form is called as string of porcelain discs. The top of the string is connected to the cross arm of the tower while the bottom of the string carried the conductors along the conduct shoe. Each disc was

designed for the lowest voltage at least 11 kV, but if they are formed as string as proper insulation, they can carry out the very high voltage levels [27]. As shown in the Figure 2.12

The dielectric strength of a string cannot be judged sufficient accurately form the flashover voltages of separate insulators and the number of each insulators in the string. This is the fact explain that the flashover distance i.e. the dry arcing distance (l_{p1}) along air between the terminal electrodes for a single disc insulator. The discharge paths of a single disc insulator and the insulator as a string are different. Flashover voltage of the string depend upon the path along which the discharge develop as shown in the Figure 2.12. Flashover along the string of insulators can divide the discharge paths which develop along the string into 3 paths [22]:

The first discharge path, along a whole the surface of the insulator in the string i.e. as the same discharge path of the single disc, but multiply with number of discs. The first discharge path can calculate with equation below:

$$L_{p1} = nl_{p1} \tag{2.5}$$

Where, *n* is the number of disc in the string

The second discharge path, along the path l_{p2} which multiply with number of discs. The second discharge path can calculate with equation below:

$$L_{p2} = nl_{p2} \tag{2.6}$$

Where, *n* also is the number of disc in the string

The third path, along the dry arcing distance of the string:

$$L_{p3} = l_{p3} \tag{2.7}$$

Average flashover gradient during the development of discharge partially or fully along the whole surfaces of the string are lower than during discharge in air, as well as the chance to occurs the flashover voltage along the path L_{p2} also to be lower than the path L_{p3} because of the L_{p3} is less than the nl_{p2} ($L_{p3} < nl_{p2}$). Hence, the

value of dry arcing distances of insulators and strings (L_{p3}) are used to simulate in this thesis.

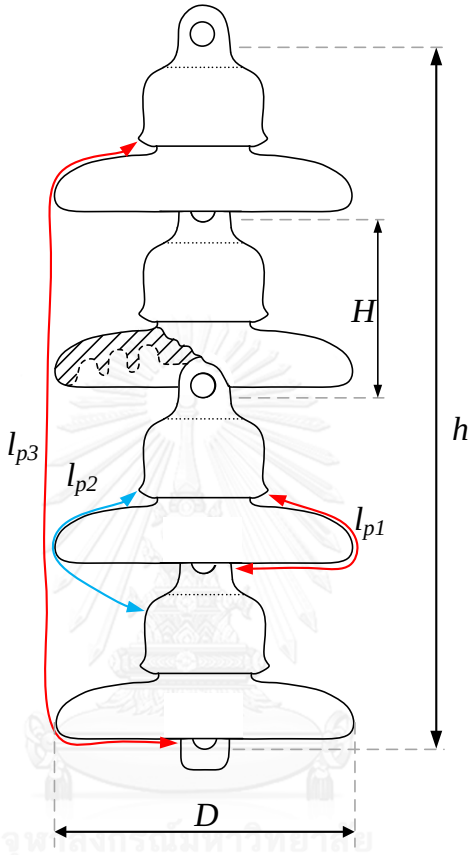

Figure 2.12 Main dimension of a string of suspension insulators

Where:

l_{p1} - Dry arcing distance of the single disc in the string.

l_{p2} - Length which measure form head insulator to another middle of head insulator in the string as figure 2.12.

l_{p3} - Dry arcing distance of the string.

H - Height of the single disc in the string.

h - Height of the string.

D - Diameter of the string or insulator

CHAPTER 3

TEST PROCEDURE AND EXPERIMENTAL RESULTS

3.1. Experimental method

The experimental results are necessary to determine model parameters and prove the simulation results. A part of experimental results, used in this thesis, received from the previous research which studied on volt-time characteristics of suspension insulators in 24 kV distribution system [14]. This research did testing for determining the critical flashover voltages (CFO), the breakdown voltages of for establishing the volt-time curves of suspension insulator strings with 1) 1 disc to 4 discs of ANSI class 52-1, 2) 1 disc to 3 discs of ANSI class 52-2, 3) 1 disc of ANSI class 52-3 and 4) 1 disc of ANSI class 52-4. Whole theses experimental results were tested under standard lightning impulse voltage (1.2/50 μs). To investigate the capability of the proposed simulation models, more tests were conducted on 3 and 4 discs of ANSI class 52-2 insulator strings under non-standard lightning impulse voltages.

The waveforms of lightning impulse voltage for establishing the volt-time characteristics follow the definition specified by IEC 60-1 [16] which the front time does not exceed 20 μs. Hence, not only the standard lightning impulse of 1.2/50 μs, a non-standard wave shape of 4.8/54.8 μs were selected for testing and simulation to verify the capability of the simulation models.

3.2. Experimental circuit

The impulse voltages are generated by discharging of high voltage capacitors through spark gaps, which act as a switch, into network resistors. Generally the voltage multiplier circuit is used. The peak value and wave shape of impulse voltages can be measured by a voltage divider with a digital oscilloscope [17].

The lightning impulse voltage tests in laboratory were performed in dry condition. As shown in the figure 3.1, the equivalent diagram of experimental circuit

consists of 5 parts: (i) Impulse generator, (ii) External load, (iii) Capacitor voltage divider, (iv) Measurement system and (v) Test object i.e. insulator or insulator string. The impulse generator capacitor C_s is charged by a high direct voltage source, then discharged over the gap *G*. The appearance of the impulse voltage across to the external resister ($R_{d,ext}$) and the load capacitor C_L . The front and tail of waveform are mainly controlled R_d and R_e, respectively. An external resistor $R_{d,ext}$ may be needed to adjust the front time of impulse voltage.

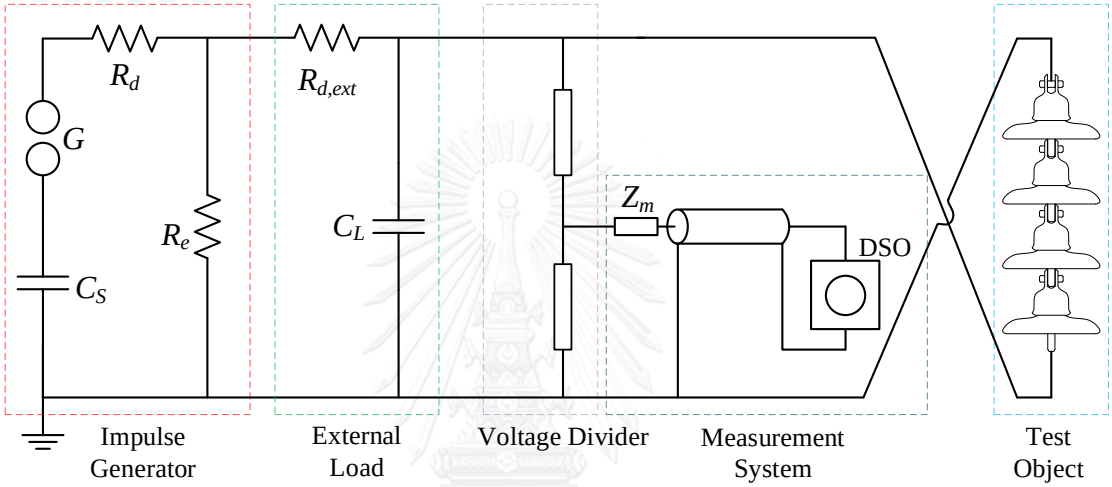

Figure 3.1 Equivalent diagram of experimental circuit

Where:

C_s - Capacitor of impulse generator,

G - Sphere gap which acts as a switch,

R_e - Resistor for front-time control,

R_d - Resistor for tail-time control,

$R_{d,ext}$ - External resistor which also adjust front wave,

C_L - Load capacitor,

Z_m - Matching impedance,

DSO - Digital storage oscilloscope.

3.3. Test objects

For the insulators which be used in this thesis to test in high voltage laboratory and to simulate with ATPDraw are the porcelain suspension insulators ANSI class 52-1

amounts 1 disc to 3 discs, ANSI class 52-2 also amounts 1 disc to 4 discs and ANSI class 52-4 amounts 1 disc. Their characteristic, dimensions and important data shown as the figure 3.2 -figure 3.7.

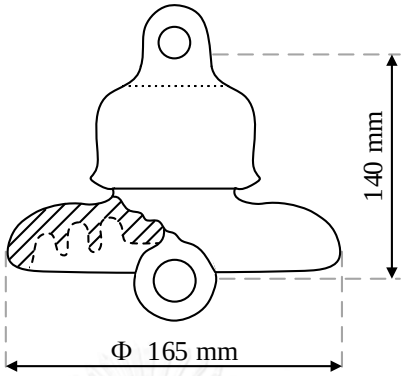

Figure 3.2 Dimension of ANSI class 52-1 insulator

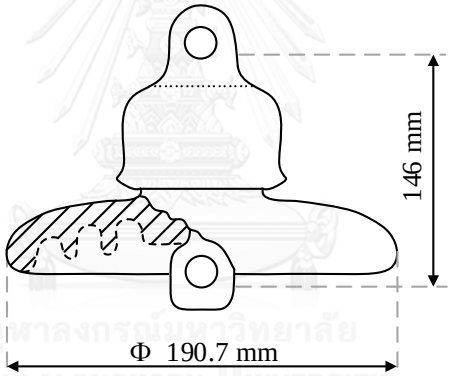

Figure 3.3 Dimension of ANSI class 52-2 insulator

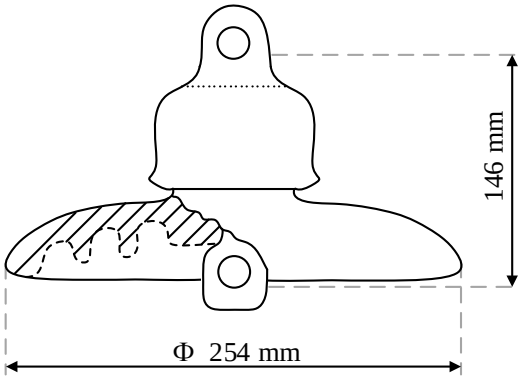

Figure 3.4 Dimension of ANSI class 52-4 insulator

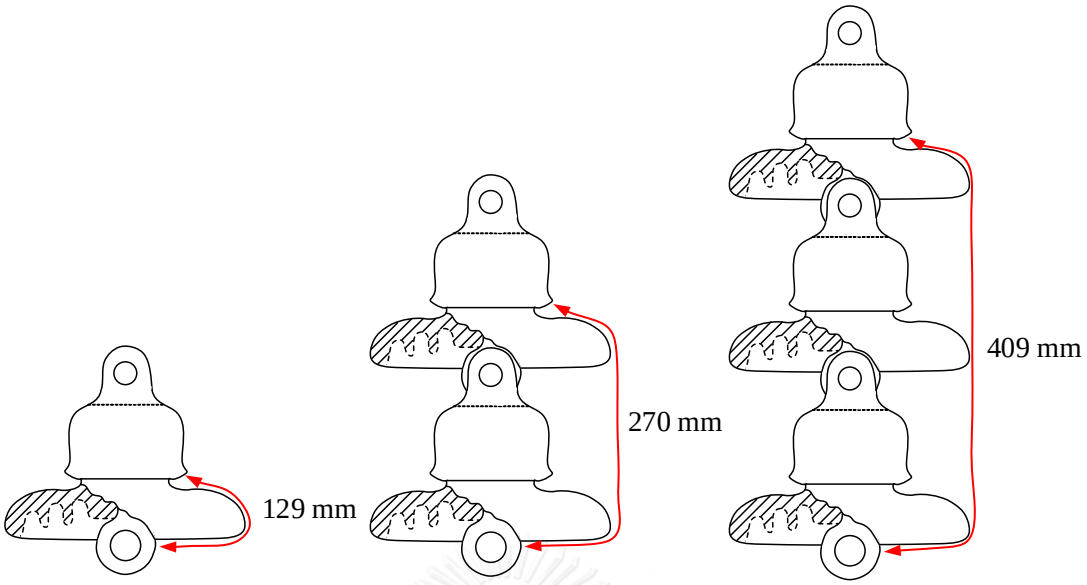

Figure 3.5 Dry arcing distances of ANSI class 52-1 insulator string (*a*) 1 disc, (*b*) 2 discs and (*c*) 3 discs

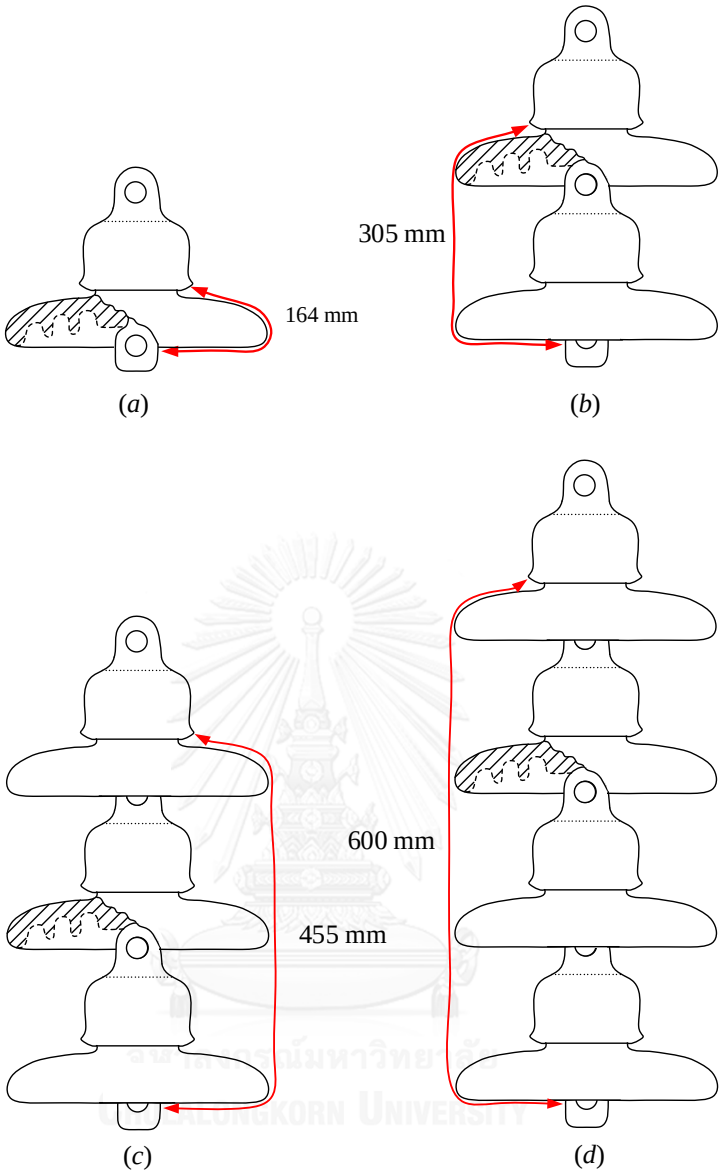

Figure 3.6 Dry arcing distances of ANSI class 52-2 insulator string (*a*) 1 disc, (*b*) 2 discs, (*c*) 3 discs and (*d*) 4 discs

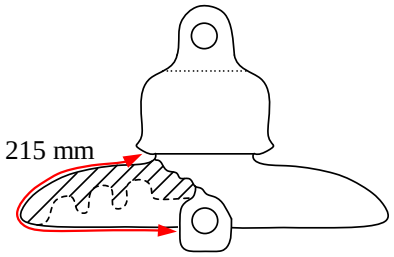

Figure 3.7 Dry arcing distances of ANSI class 52-4 insulator 1 disc

As early mentioned, ANSI class 52-1, 52-2 and 52-4 suspension insulators are investigated in this research. The dry arcing distance of insulator string, used for simulation, is determined by the shortage path in air between the top and the bottom of insulator string as shown in the figure 3.5 - figure 3.7. It depends mainly on number and height of disc. The height of disc for each insulator class are specified by ANSI standards as shown in the figure 3.2 - figure 3.4. Hence, simple formulas to estimate the dry arcing distance of insulator string (d) from the number (n) and height (H) of insulator are proposed for each insulator class.

3.3.1. For ANSI class 52-1 insulator

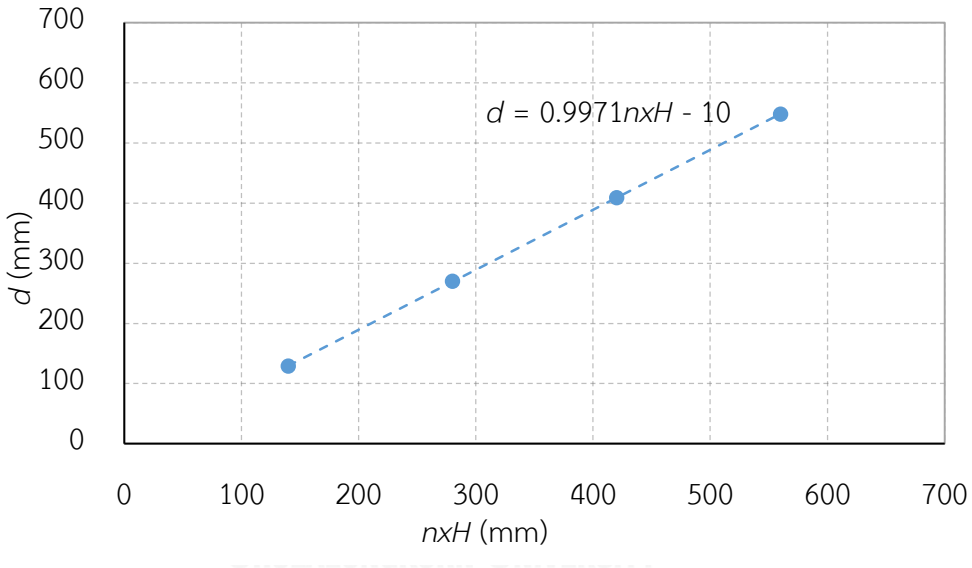

Figure 3.8 Dry arcing distance as a function of number and height of disc for ANSI class 52-1 insulator

The formula determined from the actual measurement is

$$d = 0.9971n \times H - 10 \tag{3.1}$$

It can be adjusted to be a simple formula as

$$d = n \times H - 10 \tag{3.2}$$

Where:

d - Dry arcing distance, (mm)

H - Height of the insulator, (mm)

n - Number of disc

From equation above the new estimated dry arcing distances are:

- Dry arcing distance of 1 disc is: $1\times140-10=130$ mm
- Dry arcing distance of 2 discs is: $2\times140-10=270$ mm
- Dry arcing distance of 3 discs is: $3\times140-10=410$ mm

3.3.2. For ANSI class 52-1 insulator

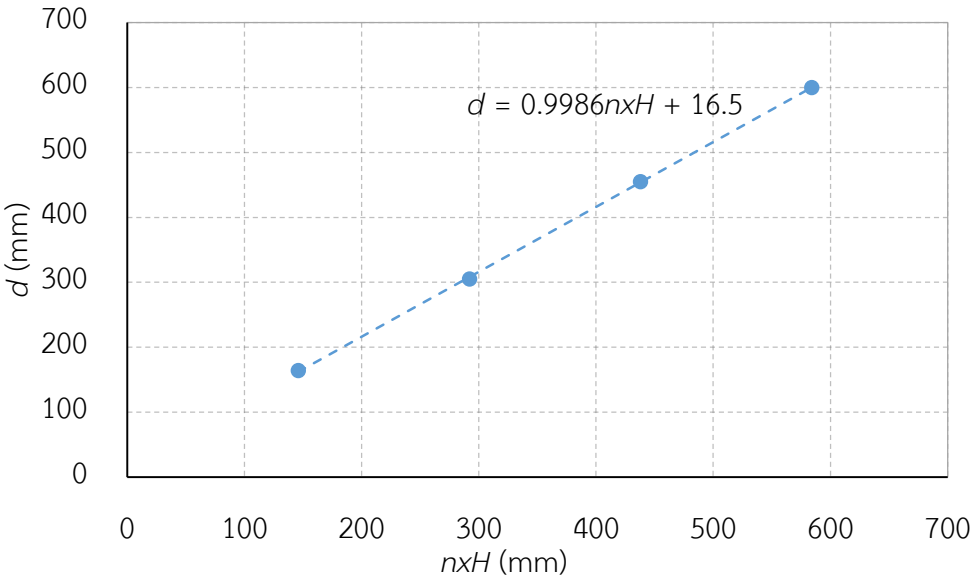

Figure 3.9 Dry arcing distance as a function of number and height of disc for ANSI class 52-2 insulator

The formula determined from the actual measurement is

$$d=0.9986n\times H+16.5 \tag{3.3}$$

It can be adjusted to be a simple formula as

$$d=n\times H+16 \tag{3.4}$$

Where:

d - Dry arcing distance (mm),

H - Height of the insulator (mm),

n - Number of disc

From the equation above the new estimated dry arcing distances are:

- Dry arcing distance of 1 disc is: $1\times146+16=162$ mm
- Dry arcing distance of 2 discs is: $2\times146+16=308$ mm
- Dry arcing distance of 3 discs is: $3\times146+16=454$ mm
- Dry arcing distance of 4 discs is: $4\times146+16=600$ mm

3.3.3. For ANSI class 52-1 insulator

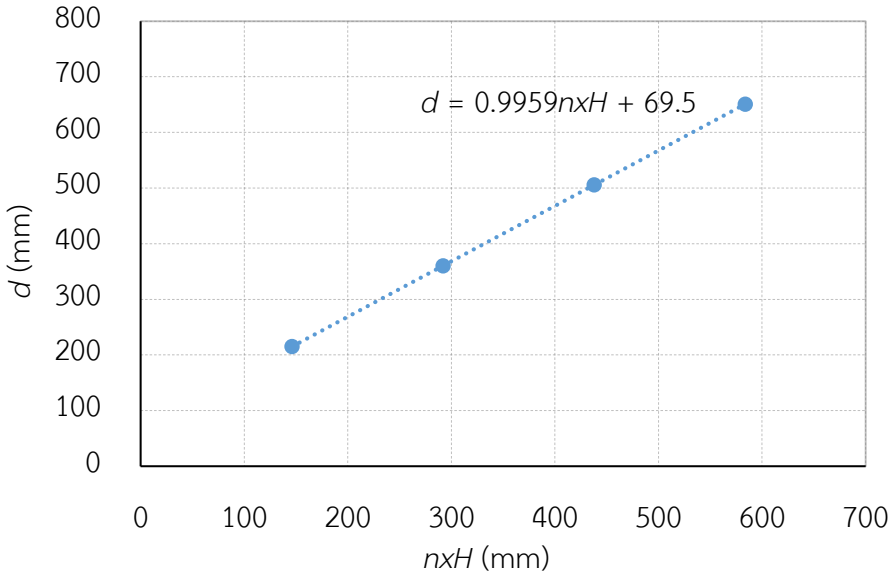

Figure 3.10 Dry arcing distance as a function of number and height of disc for ANSI class 52-4 insulator

The formula determined from the actual measurement is

$$d = 0.9959nxH + 69.5 \tag{3.5}$$

It can be adjusted to be a simple formula as

$$d = n\times H + 69 \tag{3.6}$$

Where:

d - Dry arcing distance (mm),

H - Height of the insulator (mm),

n - Number of disc

From the equation above the new estimated dry arcing distances are:

- Dry arcing distance of 1 disc is: $1\times146+69=215\ \text{mm}$

3.4. Collection data

3.4.1. Critical flashover voltages (CFO)

Table 3-1 Critical flashover voltages

Insulator	Polarity	No. of disc	$V_{50\%}$ or CFO (kV)
52-1	+	1	103.62
		2	202.48
		3	292.13
	-	1	98.41
		2	182.42
		3	265.45
52-2	+	1	121.32
		2	215.21
		3	318.11
	-	1	119.74
		2	207.47
		3	308.92
52-4	+	1	121.65
	-	1	130.92

3.4.2. Volt-time characteristics

3.4.2.1 ANSI class 52-1 insulator string

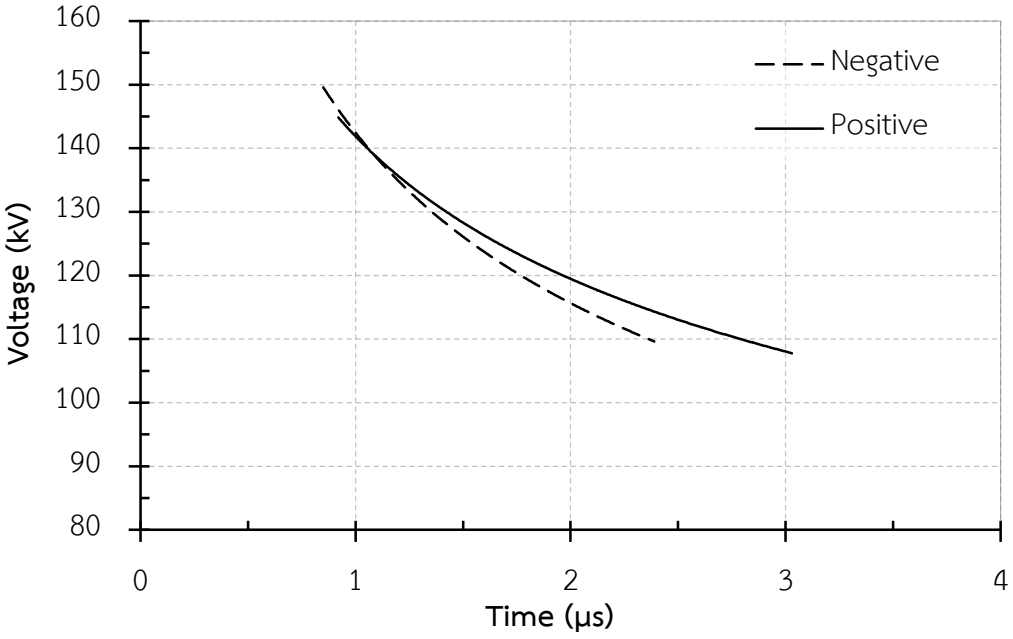

Figure 3.11 Volt-time curves of 1-disc ANSI class 52-1 insulator

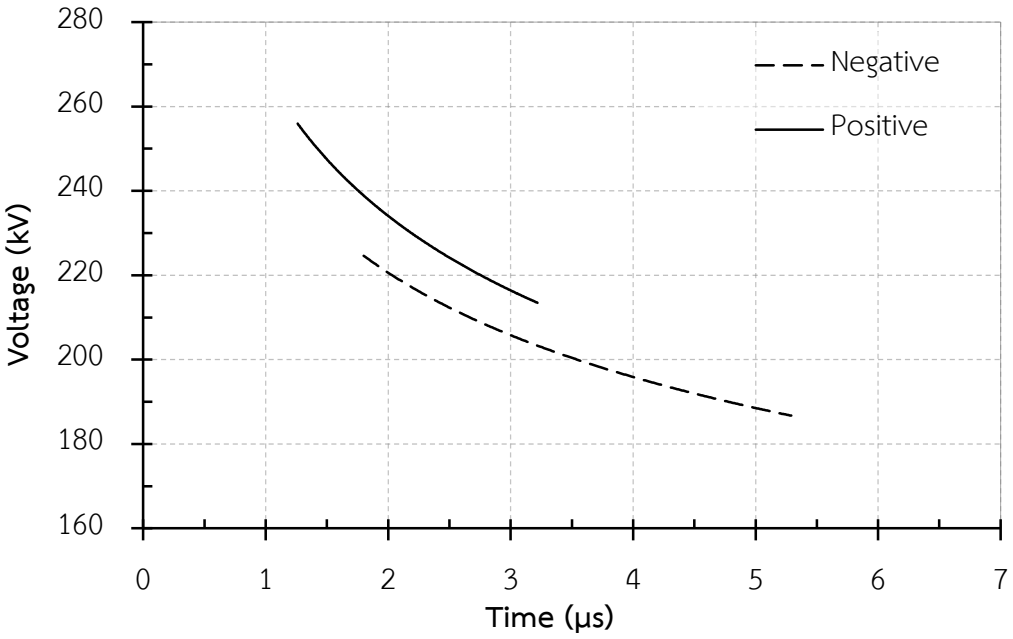

Figure 3.12 Volt-time curves of 2-disc ANSI class 52-1 insulator string

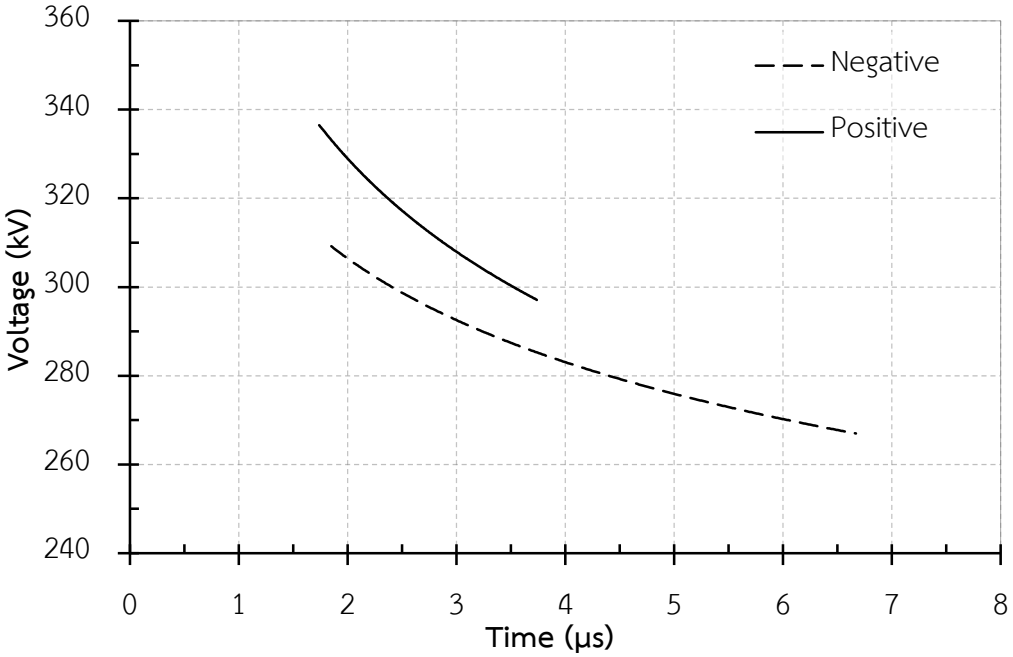

Figure 3.13 V'olt-time curves of 3-disc ANSI class 52-1 insulator string

3.4.2.2 ANSI class 52-2 insulator string

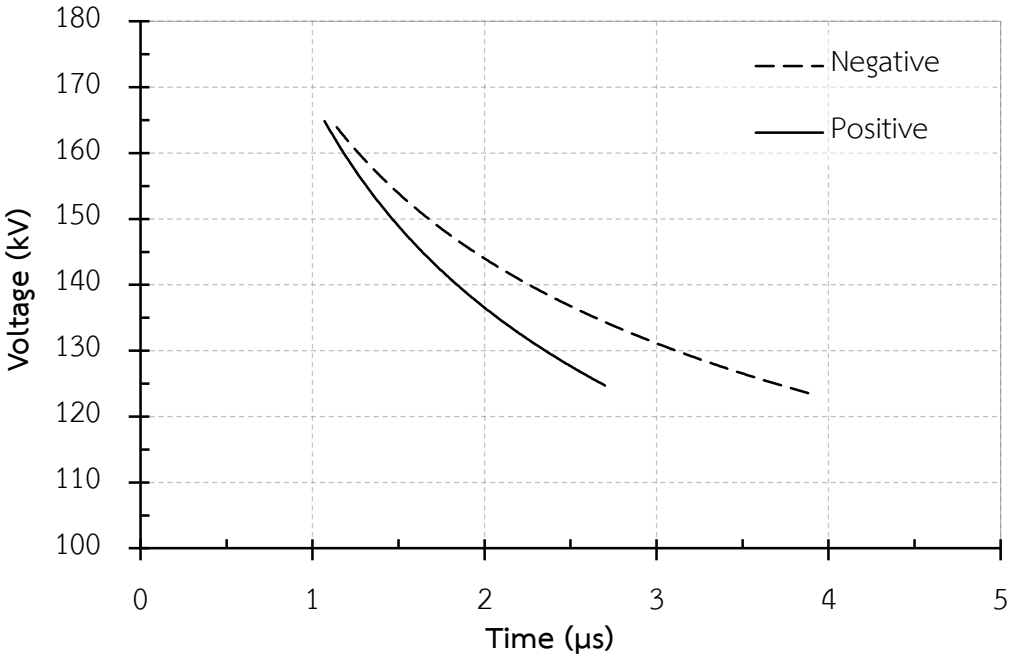

Figure 3.14 Volt-time curves of 1-disc ANSI class 52-2 insulator

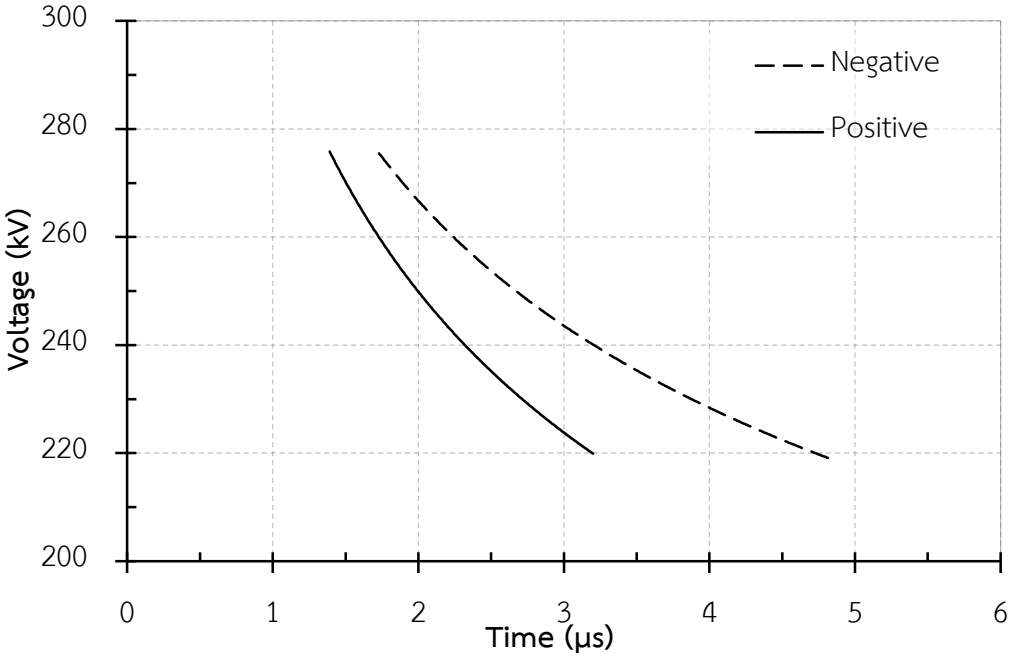

Figure 3.15 Volt-time curves of 2-disc ANSI class 52-2 insulator string

3.4.2.3 ANSI class 52-4 insulator string

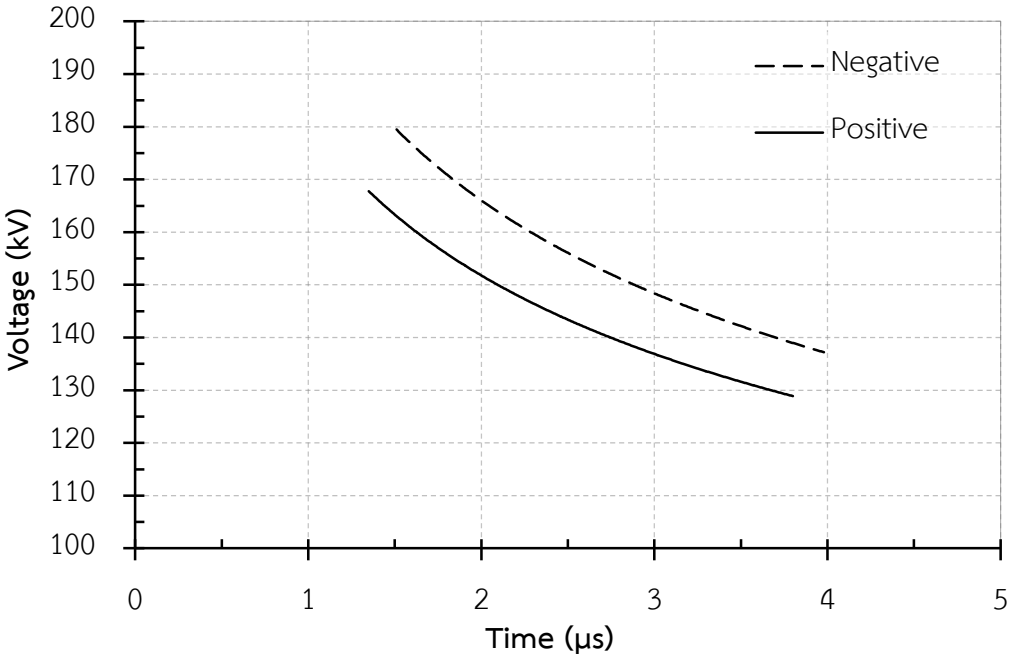

Figure 3.16 Volt-time curve of 1-disc ANSI class 52-4 insulator

3.5. Establishing the volt-time characteristics form testing

To supplement the data of volt-time characteristics of various insulator strings, more testing was conducted in this research. The volt-time characteristic was obtained by applying impulse voltages at 4-5 levels of magnitude to an insulator string. Each voltage level was applied 15 times and the corresponding time to breakdown was collected. Because the time to breakdown is random as mentioned in CHAPTER 2, the average time to breakdown was used as the representative one. It should be noted that for the case of flashover at the front of impulse, the breakdown voltage is the voltage when flashover occurs but for the case of flashover at the tail of impulse, the breakdown voltage is the peak of impulse voltage. The temperature, atmospheric pressure and absolute humidity of environment in the test area are noted to determine correction factors for transferring the breakdown voltage to standard conditions [16]. As shown in the figure 3.17, a volt-time curve is obtained by fitting the data of breakdown voltage and its corresponding time to breakdown. It can be observed that the lower breakdown voltage level, the more variation in time to breakdown.

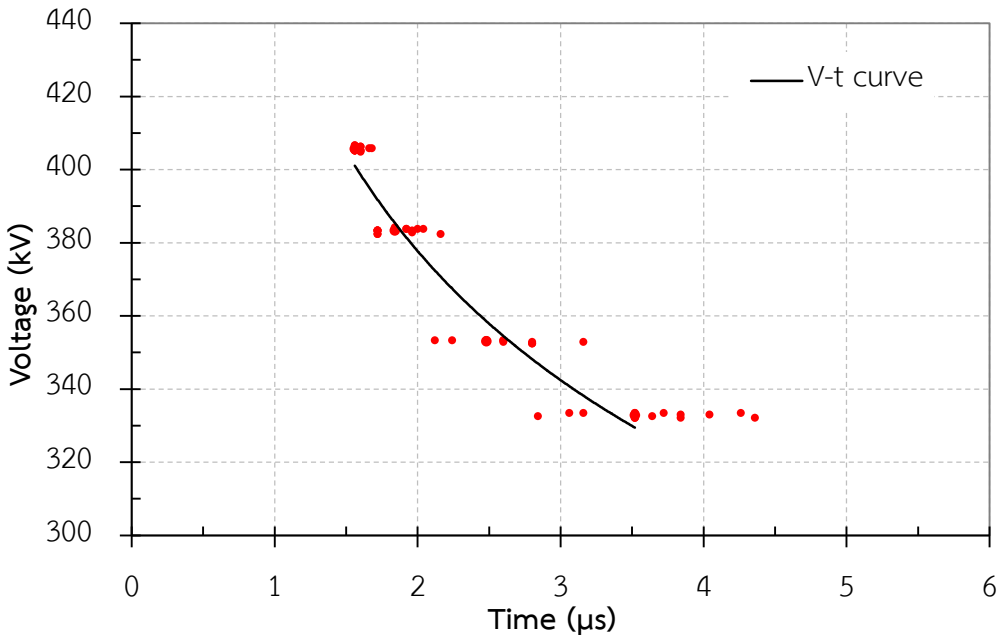

Figure 3.17 An example of distribution of chopping time for each applied voltage level

The volt-time characteristics under standard and non-standard lightning impulse voltages, obtained from the experiment in laboratory, are shown in figure 3.18 to the figure 3.21

3.5.1. Under standard lightning impulse voltages

3.5.1.1 3-disc ANSI class 52-2 insulator string

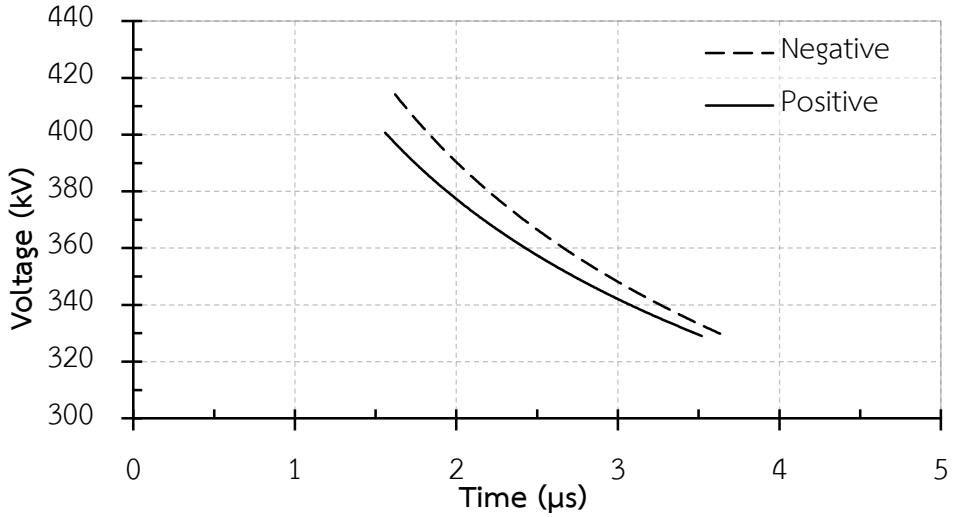

Figure 3.18 Volt-time curve of 3-disc ANSI class 52-2 insulator string

3.5.1.2 4-disc ANSI class 52-2 insulator string

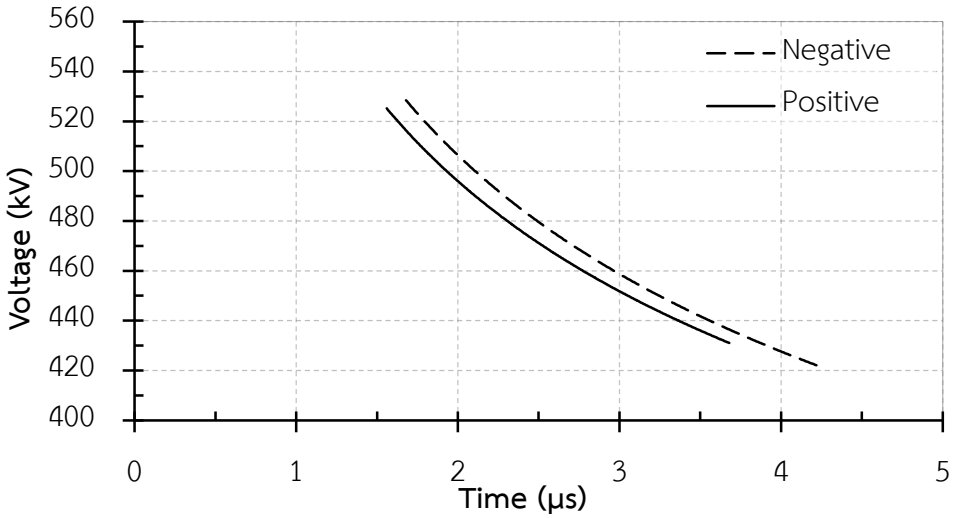

Figure 3.19 Volt-time curve of 4-disc ANSI class 52-2 insulator string

3.5.2. Under non-standard lightning impulse voltages

3.5.2.1 3-disc ANSI class 52-2 insulator string

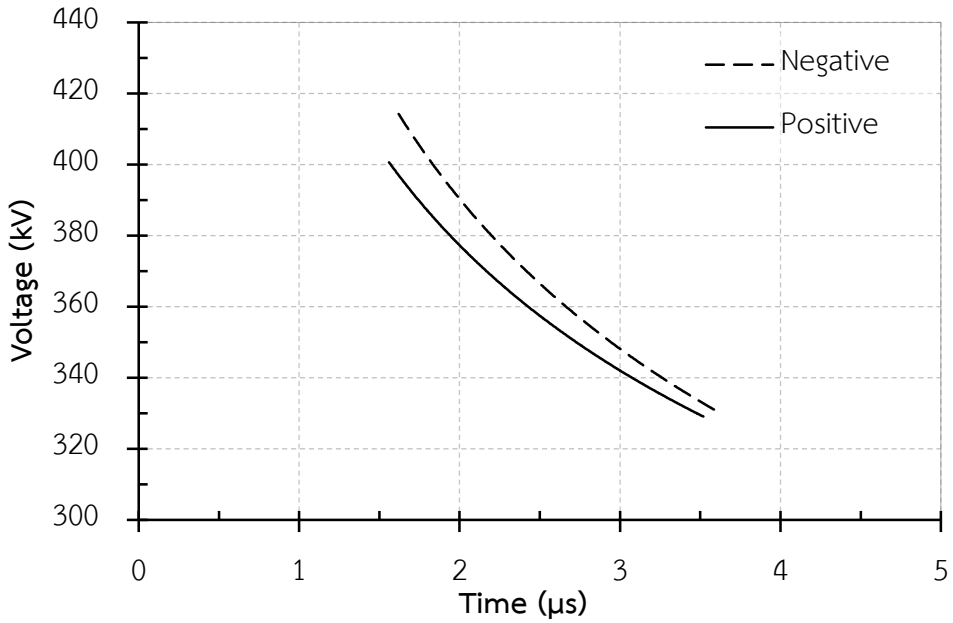

Figure 3.20 Volt-time curve of 3-disc ANSI class 52-2 insulator string

3.5.2.2 4-disc ANSI class 52-2 insulator string

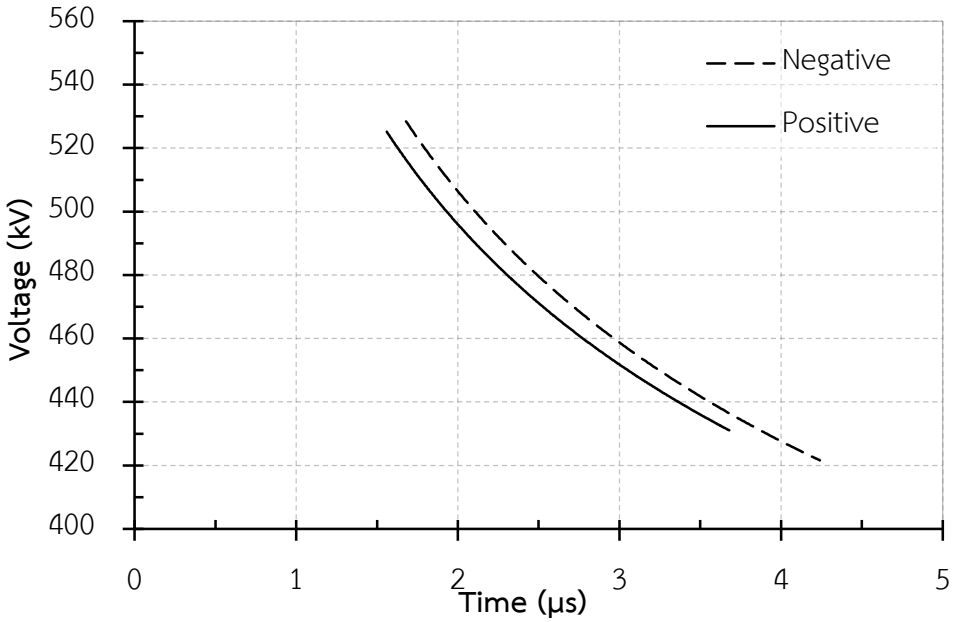

Figure 3.21 Volt-time curve of 4-disc ANSI class 52-2 insulator string

CHAPTER 4

COMPUTER SIMULATION METHOD

4.1. ATP/EMTP

The Electromagnetic Transients Program (EMTP) is considered to be one of the most widely used program for digital simulation of transient phenomena in power systems. It has been started developing in the public domain since 1984 by the EMTP development Coordination group and the Electric Power Research Institute (EPRI) of the Palo Alto, California. The Alternative Transients Program (ATP) was developed after the EMTP in the same year [13].

This digital computer cannot simulate transient phenomena continuously, they can only simulate as discrete intervals of time with a step size (Δt). By this reason, it leads to truncation errors which may be accumulated from step to step and then cause divergence form the exactly solution. Most methods used in the ATP/EMTP are numerically stable and avoid this type of error build-up [12].

The ATP calculates variables of interest within electric power systems as a function of time. Fundamentally, the trapezoidal rule of integration is used to solve the differential equation of system components in the time domain. Non-zero initial conditions can be determined either automatically by a steady-state, phasor solution or they can be entered by the user for some components. The ATP has many created models such as transformers, generators, motors, surge arresters, transmission lines and cables which consist of resistance (R), inductance (L), capacitance (C). By this digital program, complex network of arbitrary structure can be simulated. The interfacing capability to this program module TACS (Transient Analysis of Control System) and MODELS (a simulation language) is enabled to model and analysis of control systems, power electronic equipment and component with nonlinear characteristics such as electric arcs and corona discharges. Symmetric or unsymmetrical are allowed, for example, lightning surges and any kind of switching operation. As well as, dynamic

systems without any electrical network can also be simulated by using TACS and MODELS.

4.1.1. ATPDraw

ATPDraw™ for Windows OS is a graphical, mouse-driver preprocessor to the ATP version of EMTP. With ATPDraw, the user can create the circuit which need to simulate by using the mouse to point and select the components from an extensive tools. Then ATPDraw generates the input file data for the ATP simulation in the appropriate format. The circuit node names are managed by the ATPDraw but the user can give node names to the nodes of special interest.

The ATPDraw has interfaced for TACS and MODELS by connecting between self-TACS or TACS and MODELS. It can simulate network only (no TACS), TACS stand-alone (no network) and the most common use is TACS hybrid which connect both i.e. network and TACS.

4.1.2. TACS

Transient Analysis of Control System (TACS) is module for time-domain analysis of the control systems, it has been introduced in EMTP in 1976 for the simulation of HVDC converter controls. There are many functions included in TACS such as generator excitation and governor control, control loops, relaying algorithms. They can 1) simulate mechanical or electromechanical systems, 2) create models for devices without built-in MODELS e.g. arc resistances, and 3) create harmonic sources, variable frequency sources, and voltage/current source etc. TACS has been designed form point of view of reproducing Laplace domain block diagram which can be converted to difference equations, resulting in one step time delay (Δt).

4.1.3. MODELS

MODELS in ATP is a general-purpose description language supported by an extensive set of the simulation tools for the representation and study of time-variant systems. It allows the description of arbitrary user-defined control and circuit components. It also provides a simple interface for connecting other programs/models

to the ATP. As a general-purpose programmable tool, MODELS can be used for processing simulation results either in the frequency domain or the time domain. The ATPDraw supports only a simplified usage of MODELS. The user just writes a model-file and entrust the INPUT/OUTPUT section to ATPDraw.

4.2. Model with ATPDraw

TACS function and MODELS object within ATPDraw are applied to create a model for simulation of breakdown behaviors and establish the volt-time characteristics. Lightning impulse voltages with different wave shapes are created by TACS-controlled sources, and the breakdown processes are calculated with MODELS object by programmable language. MODELS will pass a signal to close the TACS-controlled switch when the breakdown occurs. The simulation circuit is shown in the figure 4.1.

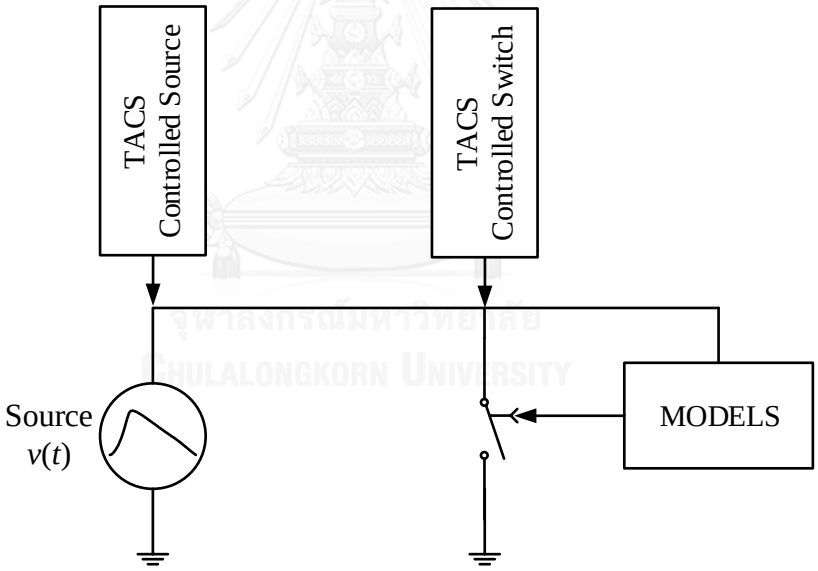

Figure 4.1 Simulation circuit

The lightning impulse voltages were generated with TACS-controlled sources by using double exponential equation below

$$v(t) = V_P \times A\left(e^{-\alpha t} - e^{-\beta t}\right) \tag{4.1}$$

Where:

V_P - Required peak value of impulse voltage (kV)

A - A constant proportional to peak of impulse voltage

α - A constant specifying falling slope (s^{-1})

β - A constant specifying rising slope (s^{-1})

t - Time (s)

For the lightning impulse voltage of standard wave shape (1.2/50 μs), the value of each parameter is as follows: $\alpha = 1.4663 \times 10^4$, $\beta = 2.4691 \times 10^6$ and $A = 1.0373$ [12]. As shown in figure 4.2, the simulated waveform is similar to the actual impulse voltage generated for experiments. For the non-standard lightning impulse voltage of 4.8/54.8 μs, the value of each parameter is adjusted as follows: $\alpha = 1.5485 \times 10^4$, $\beta = 4.8865 \times 10^5$ and $A = 1.1562$. The lightning impulse waveforms of 1.2/50 μs and 4.8/54.8 μs, created by TACS-controlled source for simulation, are shown in figure 4.3 and figure 4.4.

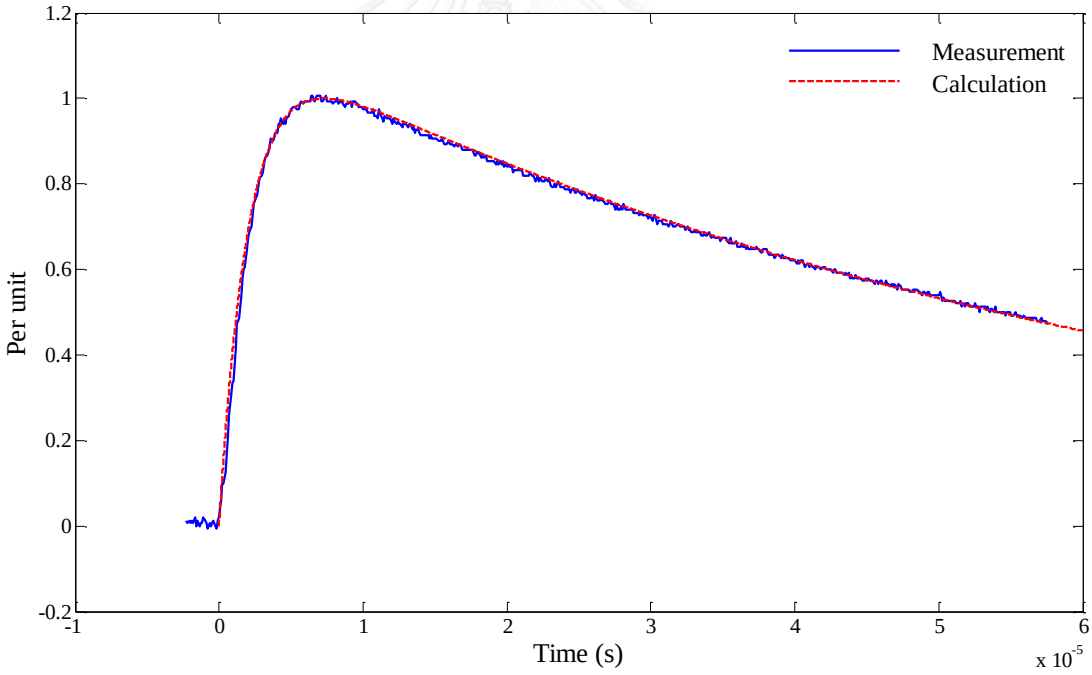

Figure 4.2 The comparison of lightning impulse between experiment and simulation

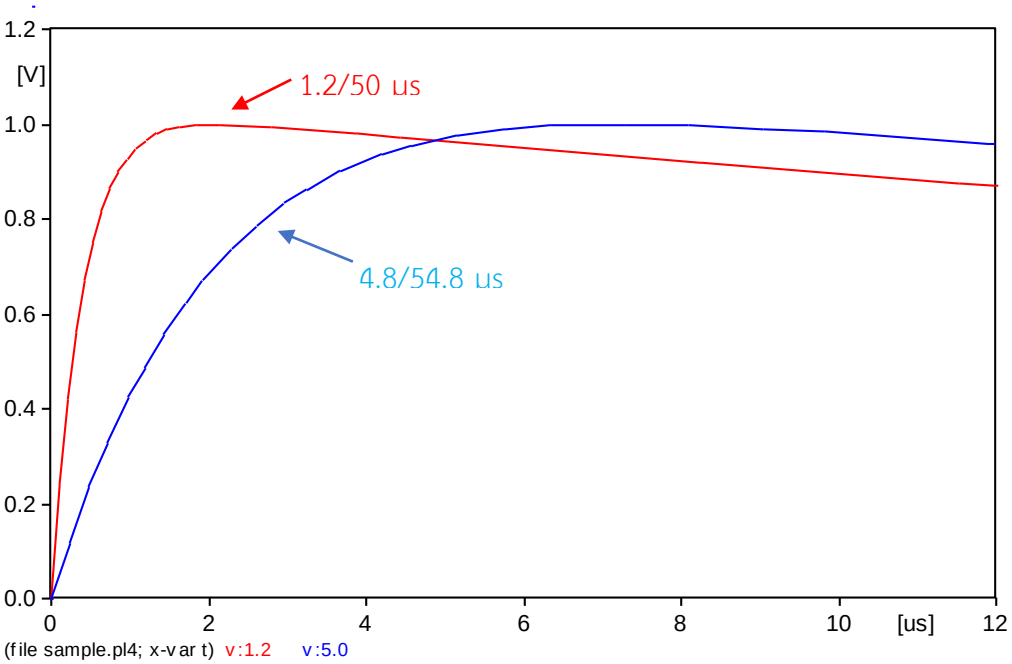

Figure 4.3 Front wave shape of simulated lightning impulse voltages

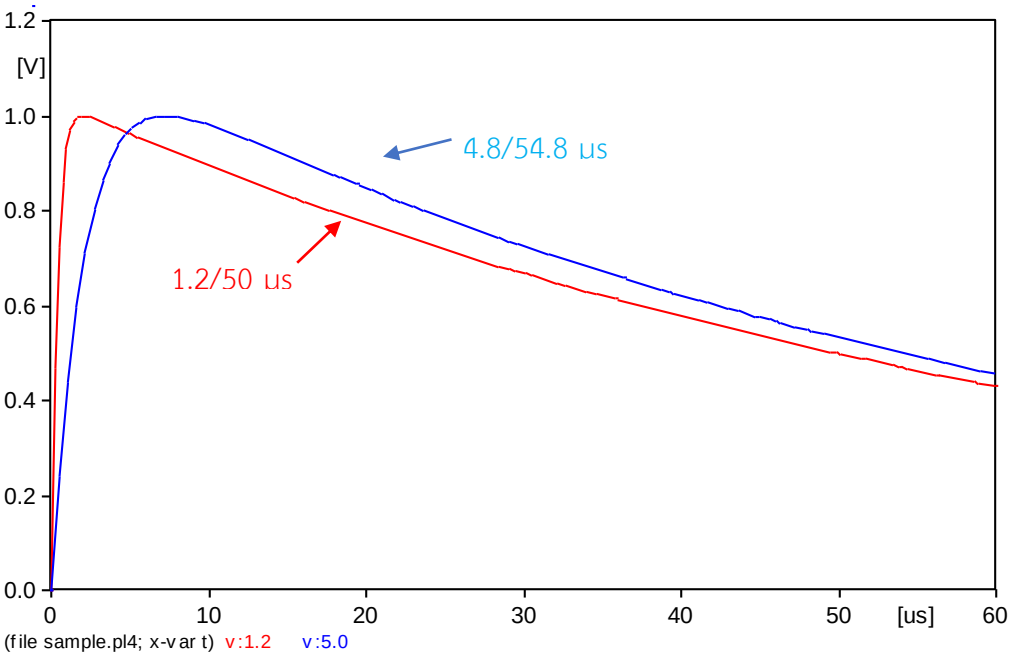

Figure 4.4 Tail wave shape of simulated lightning impulse voltages

4.3. Simulating of the insulator strings

4.3.1. Integration method (IM)

The integration method is based on the development of impulse voltage until the specific accumulating area under waveform reaches a constant called the disruptive effect (*DE*). The breakdown depends on both voltage magnitude and its appearance duration as shown in equation (5.1) and Figure 4.5.

$$DE = \int_{t_0}^{t_b} \left[V(t) - V_0 \right]^k dt \tag{4.2}$$

Where:

$V(t)$ - Applied voltage as function of time

V_0 - Onset voltage, i.e. the minimum voltage which must be exceeded before any breakdown process can start

t_0 - Time to start integrate when $V(t) \geq V_0$

t_b - Time-to-breakdown

k - Empirical constant

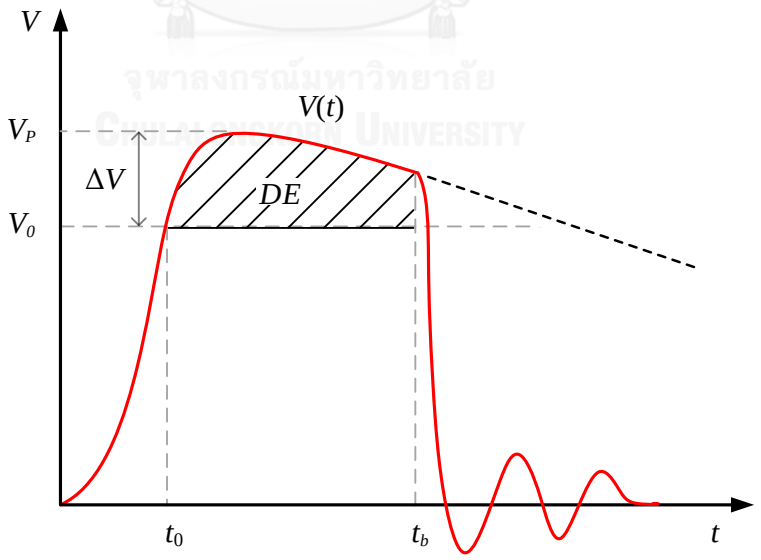

Figure 4.5 Integration method

It is assumed that *DE** is a characteristic of the insulation configuration and is independent of the wave shape of the applied voltage. Then, it is obvious from equation (5.1) that V_0 and *k* are not independent constants. In [29], this inter-dependence is examined. If V_0 is small (e.g. $0 \le V \le V_{50\%}$), *k* is large (in the range 3 to 5). If V_0 is large (~ 90% of $V_{50\%}$), $k \le 1$. In the empirical formulation of the integration method, there is a need for guidance in the selection of V_0 and *k* based on any knowledge of the physical process involving in the breakdown. Rather the set of value for DE^*, V_0 and *k* is chosen simply on their capacity to provide the best fit between the estimated and measured standard wave shape volt-time characteristics. Of course, if $k=1$, then we have the simpler version as equation, which is the equal-area criterion.

$$DE = \int_{t_0}^{t_b} [V(t) - V_0]\, dt \tag{4.3}$$

Therefore, this method was developed in many models. For example, the models of Sekioka [10] and Wanit [28] as shown in the following equations.

❖ Model of Sekioka

Sekioka defined *k* = 1 and V_0 = ~90% of $V_{50\%}$. *DE* equations of Sekioka model were determined by the arcing horns rod-rod gaps length d in m.

Positive polarity: $DE = 0.65d - 0.04$ (4.4)

Negative polarity: $DE = 0.61d - 0.15$ (4.5)

❖ Model of Wanit

Wanit modified the *DE* equation of Sekioka to simulate breakdown characteristics of arcing horns rod-rod short air gaps for distribution power transformer's bushing 22kV and 33 kV.

Positive polarity: $DE = 0.3705d - 0.0014$ (4.6)

Negative polarity: $DE = 0.5173d - 0.0144$ (4.7)

Both models of Sekioka and Wanit were developed for breakdown simulation for arcing horn rod-rod gaps. Thus, for suspension insulator strings, the new equations for determining DE shall be proposed. This can be done by solving the integration equation (5.2). Where $V(t)$ follows equation (3.1) as standard lightning impulse of 1.2/50 μs, V_0 is set to 90% of $V_{50\%}$, t_0 is the time to start integration when $V(t) \geq V_0$ and t_b is the time lead to breakdown. Then bring each result of DE calculated from equation (5.2) to plot versus their corresponding dry arcing distance d as shown in figure 5.2. Finally the equation for determining DE as a function of dry arcing distance for suspension insulator strings with ANISI class 52-2 1-4 discs as shown in equations (5.7) and (5.8).

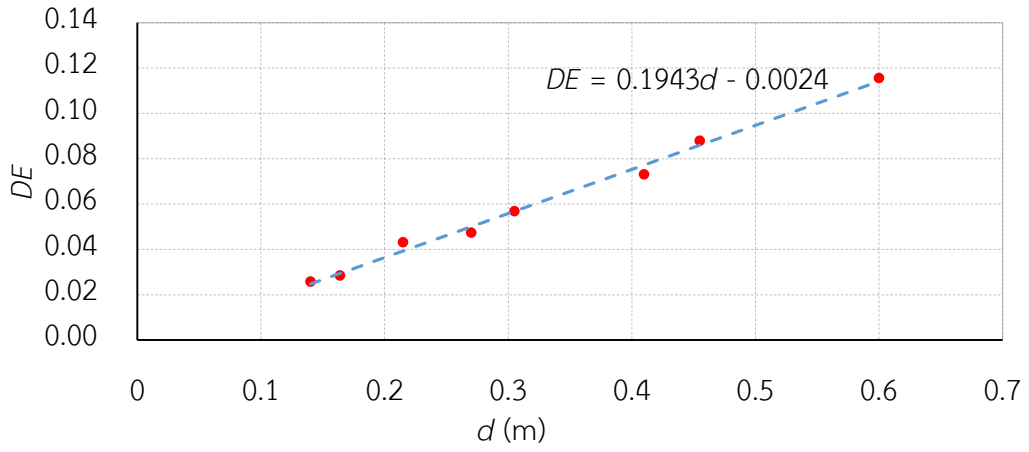

(*a*) Positive polarity

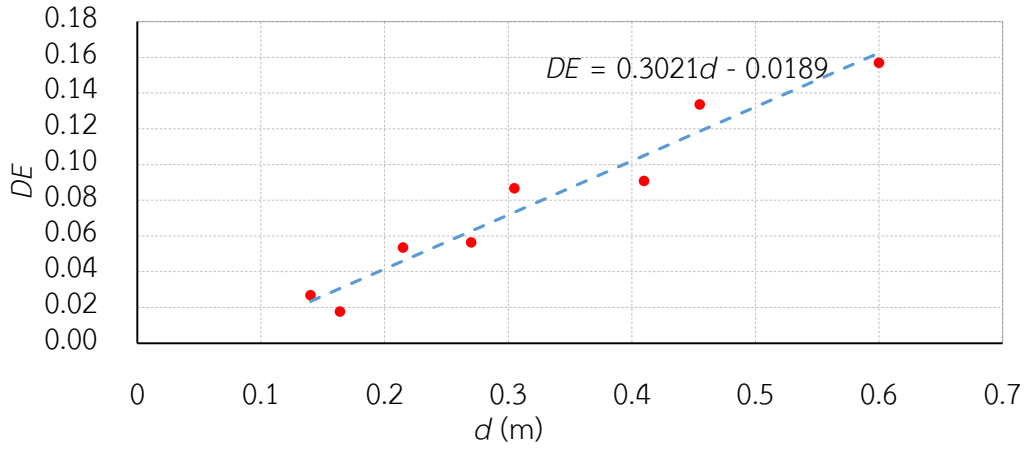

(*b*) Negative polarity

Figure 4.6 *DE* equation for (*a*) Positive polarity and (*b*) Negative polarity

The *DE* equations of breakdown simulation for suspension insulator string are:

Positive polarity: $DE = 0.1943d - 0.0024$ (4.8)

Negative polarity: $DE = 0.3021d - 0.0189$ (4.9)

Where: d – Dry arcing distance [m]

The flowchart of breakdown simulation with ATP based on integration method is shown in the figure 4.7

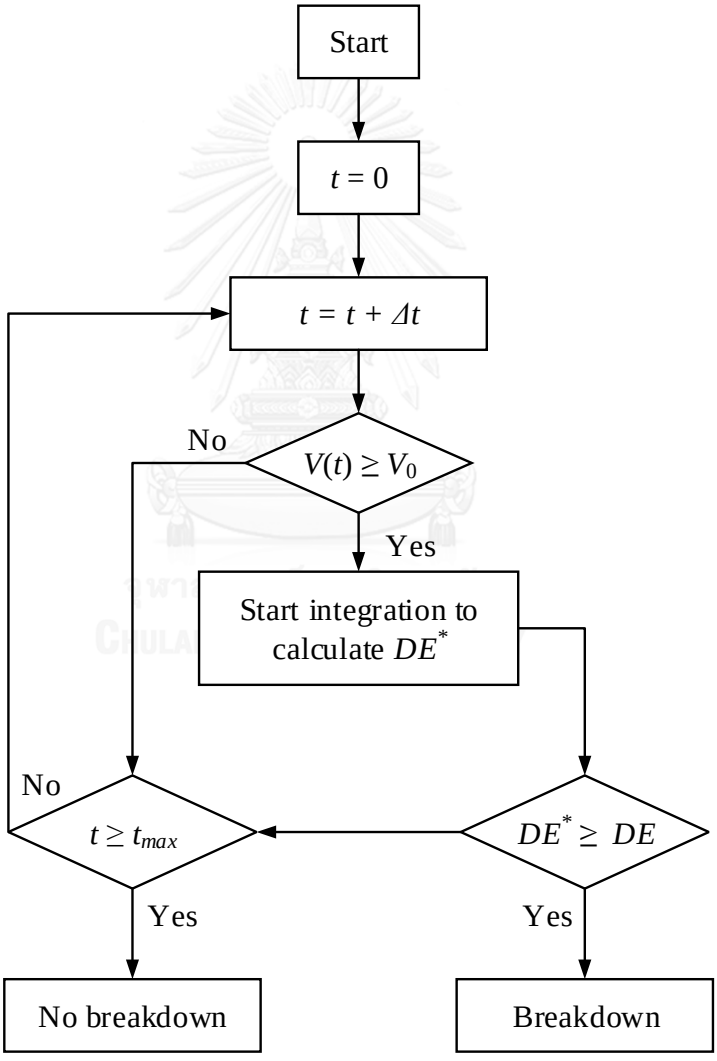

Figure 4.7 Integration method's breakdown flowchart

4.3.2. Leader progression model (LPM)

The development of the leader method was proposed by CIGRE [3]. It is based on the physical breakdown process. The time which leads to breakdown consist of three parts of time: corona inception time, streamer propagation time and leader propagation time. Hence, form ref. [4], the time to breakdown or chopping time (t_c) can be defined by the equation below

$$t_c = t_i + t_s + t_l \tag{4.10}$$

Where:

t_i - Corona inception time, usually it is neglected because it is very short duration compared with the two other times,

t_s - Streamer propagation time (μs),

t_l - Leader propagation time (μs),

For t_s can be calculated by the equation below

$$\frac{1}{t_s} = 1.25\left(\frac{E}{E_{50}}\right) - 0.95 \tag{4.11}$$

Where:

E - Maximum gradient at gap before breakdown, (kV/m)

E_{50} - Average gradient at CFO, (kV/m)

And for t_l can obtain from the equation below

$$Ve = \frac{dL}{dt} = Kv(t)\left[\frac{v(t)}{d-L} - E_0\right] \tag{4.12}$$

Where:

Ve - Velocity of the leader (m/s),

$v(t)$ - Voltage as a function of time (kV),

L - Leader length (m),

d - Dry arcing distance or gap length (m),

E_0 - Gradient at which the breakdown process start (kV/m),

K - Constant value.

According to refs. [4-7], a lightning impulse $v(t)$ is applied to an insulator string with a distance *d*. The process of the leader will start when the voltage gradient has been greater than the critical value E_0. As this process, the front wave shape of lightning impulse increases sharply and the velocity of leader (*Ve*) also travels very quickly. They affect to the leader length (*L*). Subsequently, the leader starts propagating along the insulator string distance (*d*) until it reaches the opposite electrode which means that the leader length and the dry arcing distance of insulator string are equal. At this moment, the leader progressively bridges the wholes terminal electrodes of the insulators string, then the flashover occurs. On the other hand, if the average electric field strength is lower than the critical value E_0, the leader cannot develop and the flashover won't occur. The development of the leader depends upon the arcing distance, insulator string configuration, and the polarities of the applied lightning impulse. The breakdown process of LPM is shown in the figure 4.8.

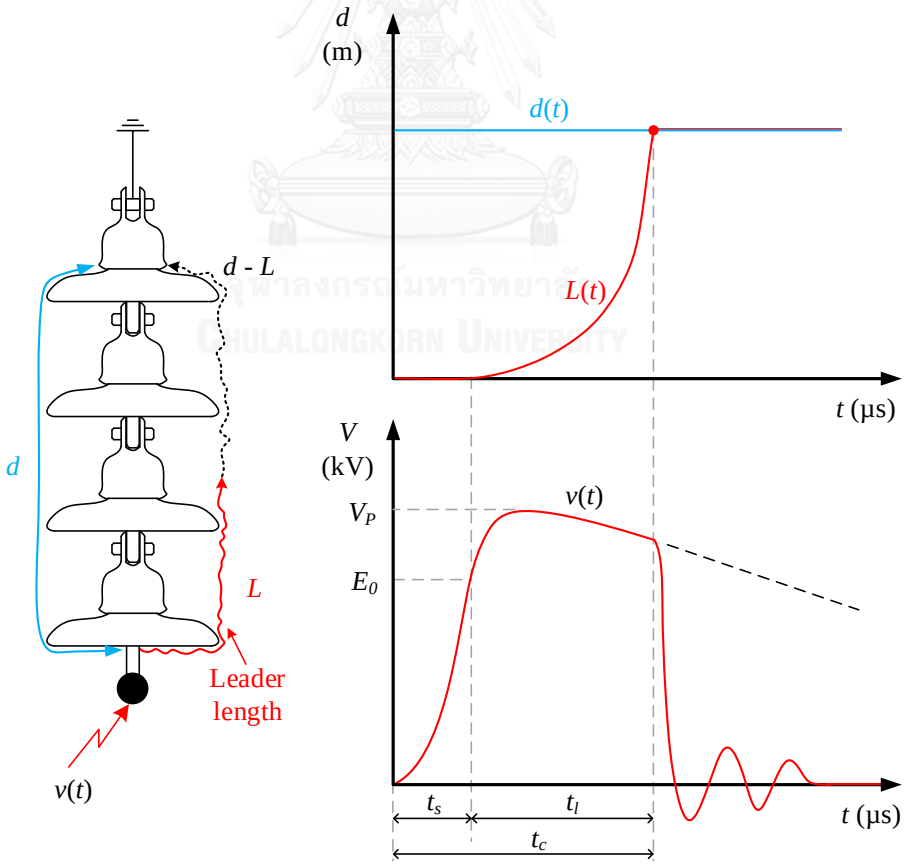

Figure 4.8 The development of leader and the breakdown process

The flowchart of breakdown simulation with ATP based on leader progression model is shown in figure 4.9.

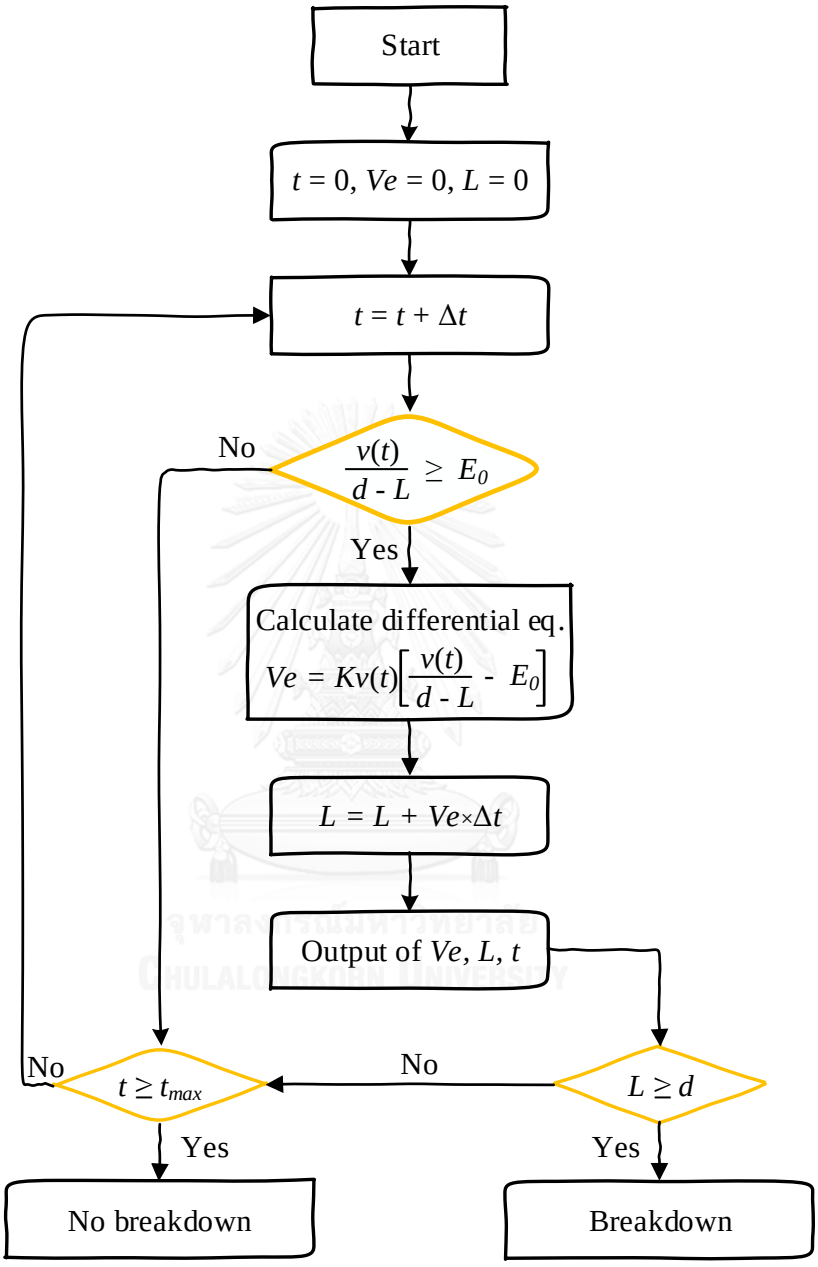

Figure 4.9 Leader progression model's breakdown flowchart

There are two constant values in the equation (5.11) i.e. K and E_0. The constant values K and critical value E_0 depend on the insulator strings configuration, type of the insulators discs and the polarities of the lightning impulse voltages. The basic guideline

of IEEE transient working group [4] and ref. [5] offered these values as shown in table 4-1 and table 4-2.

Table 4-1 The constant values of *K* and E_0 proposed in ref. [4]

Configuration	Polarity	$K\left(\frac{\mathrm{m}^2}{\mathrm{kV}^2\mathrm{sec}}\right)$	$E_0\left(\frac{\mathrm{kV}}{\mathrm{m}}\right)$
Air Gaps, Post insulators	Positive	0.8	600
	Negative	1.0	670
Cap and Pin Insulators	Positive	1.2	520
	Negative	1.3	600

Table 4-2 The constant values of *K* and E_0 proposed in ref. [5]

Configuration	Polarity	$K\left(\frac{\mathrm{m}^2}{\mathrm{kV}^2\mathrm{sec}}\right)$	$E_0\left(\frac{\mathrm{kV}}{\mathrm{m}}\right)$
Air Gaps with rod-rod arcing horn	Positive	0.6474	578

Using LPM, this thesis needs to create a model to simulate the breakdown behavior and establish the volt-time characteristics of insulators strings with various suspension insulators types such as ANSI class 52-1, ANSI class 52-2 and ANSI class 52-4, each string consists of various number of discs. Dry arcing distance (*d*) is defined as a discharge path which in a relationship between the number of discs and height (*H*) of suspension insulator string as show in equation (3.2), (3.4) and (3.6). As mentioned, the constant values of *K* and E_0 depend on insulator configuration, the insulators type and the polarity of lightning impulse. In this thesis the new constant values of *K* and E_0 are proposed from the experimental results. They are shown in table 4-3.

Table 4-3 The constant values of *K* and E_0 for model

Insulator ANSI class	Polarity	$K\left(\frac{\mathrm{m}^2}{\mathrm{kV}^2\mathrm{sec}}\right)$	$E_0\left(\frac{\mathrm{kV}}{\mathrm{m}}\right)$
52-1	Positive	3	750
	Negative	2.6	680
52-2	Positive	2.4	700
	Negative	1.6	690
52-4	Positive	3	580
	Negative	2.1	600

4.4. IM & LPM model with ATPDraw

For convenience in the simulation, both IM and LPM are created as a component with MODELS and TACS in ATPDraw as shown in figure 5.6. User just inputs the required parameters of each model to simulate the breakdown of insulator string.

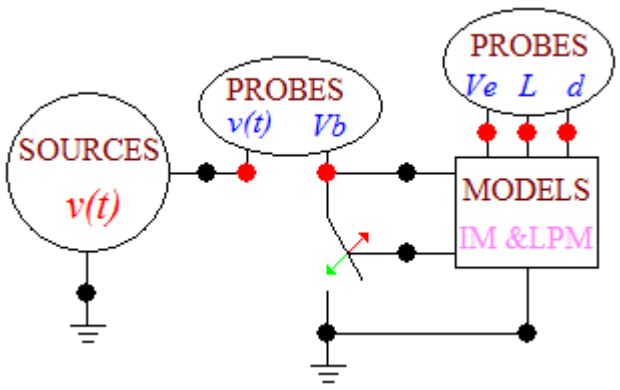

Figure 4.10 IM & LPM model with ATPDraw

Attributes

DATA	UNIT	VALUE
VP	kV	210
LIS	[1-2]	1

NODE	PHASE	NAME
TACS	1	vt
To	1	

Figure 4.11 Input data for Sources

Where:

VP - Peak voltage of lightning impulse.

LIS - Lightning impulse selector (1-2). Standard lightning impulse and Non-standard lightning impulse respectively.

DATA	UNIT	VALUE
n	Disc(s)	1
CFO	kV	100
DES	[1-2]	1
K	m^2 /kV^2.s	3
E0	kV/m	750
IS	[1-5]	1
MS	[1-2]	1

NODE	PHASE	NAME
VT	1	Vb
VN	1	
Ve	1	Ve
L	1	L
d	1	d
T_Switch	1	XX0001

Figure 4.12 Input data for IM & LPM MODELS

Where:

n - Number of disc.

CFO - Critical flashover voltage for IM.

DES - DE equation selector (1-2): DE equation for positive polarity and negative polarity of lightning impulse, respectively.

K - Constant value for LPM.

E0 - Critical electric field for LPM.

IS - Insulator selector (1-5): ANSI class 52-1, 52-2, 52-4, 52-4 with arcing horn rod-rod and 52-4 with arcing horn sphere-sphere, respectively.

MS - Model selector (1-2): Integration method (IM), Leader progression model (LPM), respectively

4.4.1. Integration method with ATPDraw

TACS function and MODELS object within ATPDraw [13] are used to create the model according to the flow chart shown in the figure 4.7. The lightning impulse voltages are generated by a TACS-controlled source. When the time-varying impulse voltage (V_t) becomes higher than V_0 (90% of $V_{50\%}$), the integration device of TACS starts integration until its output reaches the value of *DE* which is calculated from equation (5.7) or (5.8). The maximum value of the voltage reached (V_b) and the final time of integration or the time to breakdown (t_b) are recorded. The case of breakdown are shown figure 4.13 and the case of no breakdown are shown figure 4.14

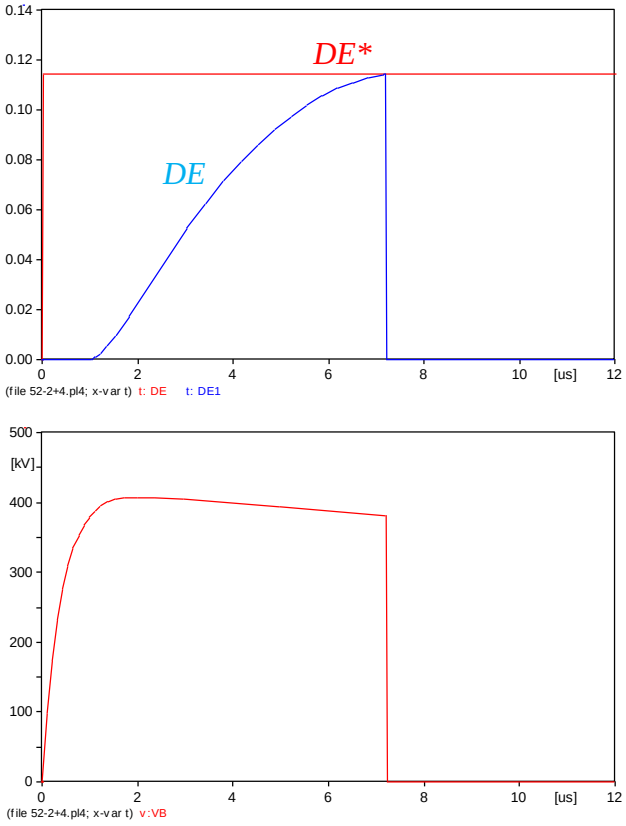

Figure 4.13 Case of breakdown in with integration method in ATPDraw

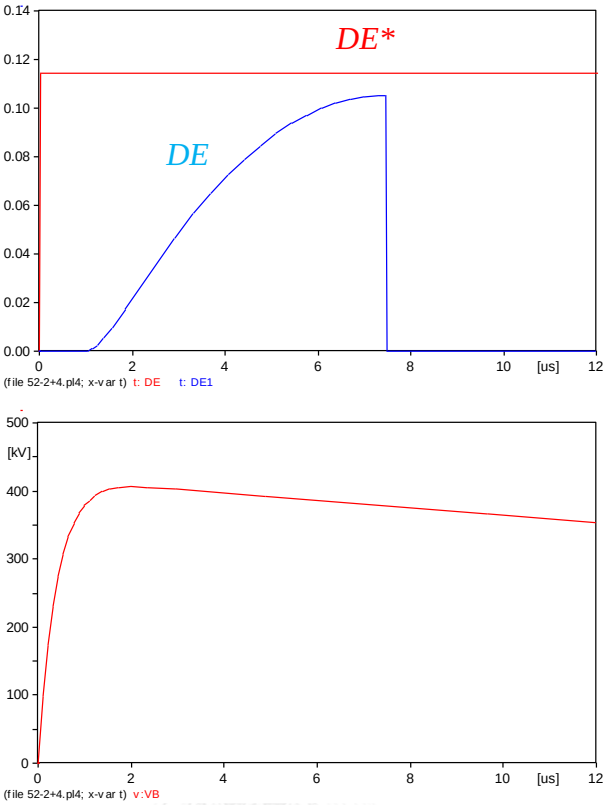

Figure 4.14 Case of no breakdown in with integration method in ATPDraw

4.4.2. Leader progression model with ATPDraw

TACS function and MODELS object within ATPDraw [13] are used to create the model as shown in the figure 4.10. According to the figure 4.8 and the flow chart as shown in Figure 4.9, a lightning impulse voltage is generated by a TACS-controlled source. A time, velocity and length of leader start at zero. Then, the time is varied by the step-time (Δt). When the time start varying, the voltage gradient $\left(v(t)/(d-L)\right)$ in the unbridged part of the gap become greater than E_0, the MODELS start calculate the velocity of leader by differential equation (5.11), while the velocity has increased rapidly, the length of leader was increased by the velocity multiply with the step-time (Δt). If the leader length has been greater than or equal the dry arcing distance of an insulator string, that mean breakdown. If not yet, and the time already has reached the maximum of time (t_{max}) which set in ATPDraw, in this case is no breakdown, try to add more the magnitude of lightning impulse voltage. The case of breakdown are shown in the figure 4.15 and the case of no breakdown are shown in the figure 4.16.

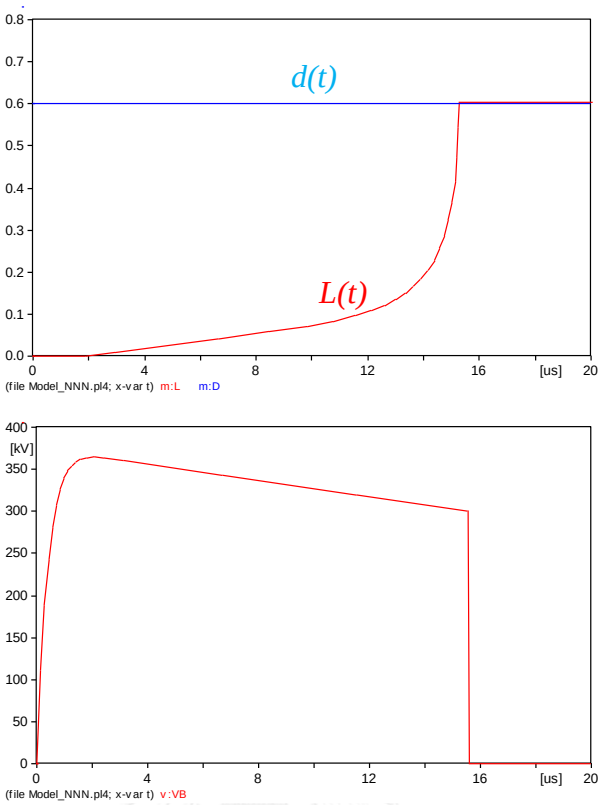

Figure 4.15 Case of breakdown in with LPM in ATPDraw

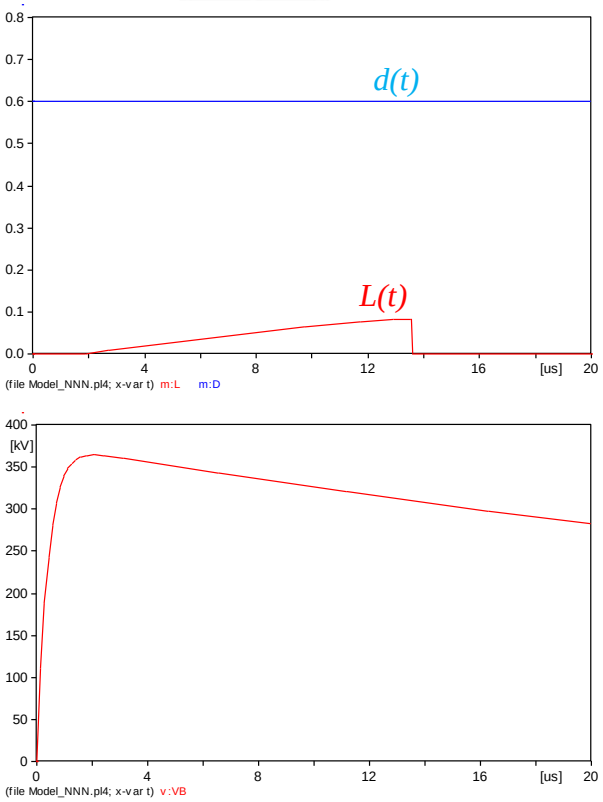

Figure 4.16 Case of no breakdown in with LPM in ATPDraw

The cases of no breakdown of LPM, observe that the leader length developed slowly and decayed to zero suddenly because of the voltage gradient become greater than E_0 but cannot steady enough to bring the leader length until reach the dry arcing distance.

The cases of breakdown of LPM, observe that the leader length has developed continually until reach the dry arcing distance. The maximum value of the voltage which cause the breakdown is breakdown voltage and the final time of leader length which reached dry arcing distance is time to breakdown or chopping time.

By varying the magnitude of input impulse voltage at TACS-controlled source, it provided some values of the breakdown voltage (V_b) and their corresponding time-to-breakdown (t_b) or chopping time (t_c), both are noted and plot in the Microsoft Excel. Hence, the volt-time characteristics of an insulator strings are obtained by number of this process which lead to breakdown. The volt-tine characteristic which got from the IM & LPM model shown in the figure 4.17.

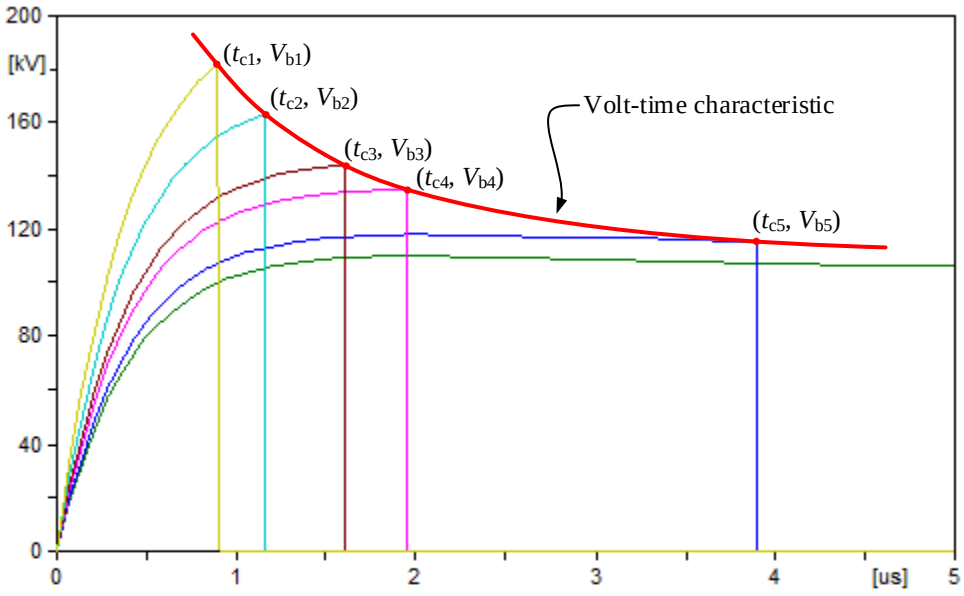

Figure 4.17 Volt-time characteristic from the IM & LPM model

CHAPTER 5

SIMULATION RESULTS AND ANALYSIS

5.1. Results and comparisons of volt-time characteristics

5.1.1. Case of standard lightning impulse (1.2/50 μs)

5.1.1.1 ANSI class 52-1 insulators string

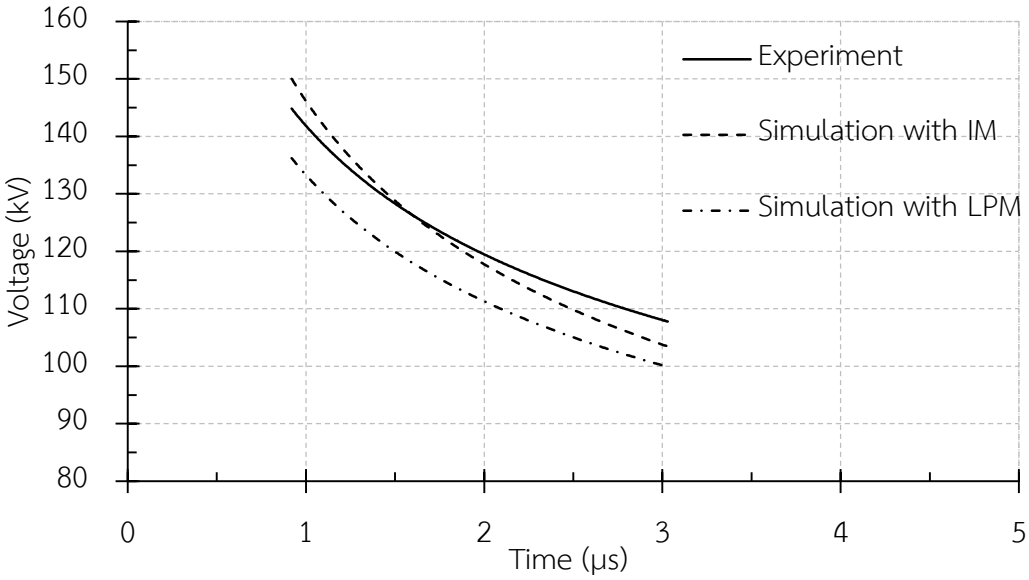

(*a*) Positive polarity

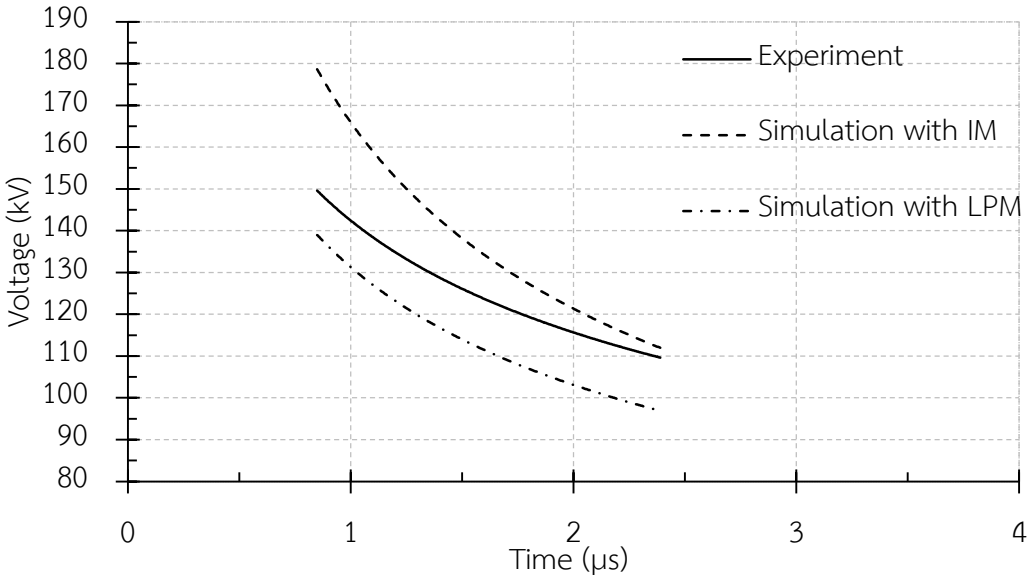

(*b*) Negative polarity

Figure 5.1 The comparison between volt-time characteristics which obtained from experiment and simulation of 1-disc ANSI class 52-1 insulator under standard lightning impulse voltages of (*a*) Positive polarity and (*b*) Negative polarity

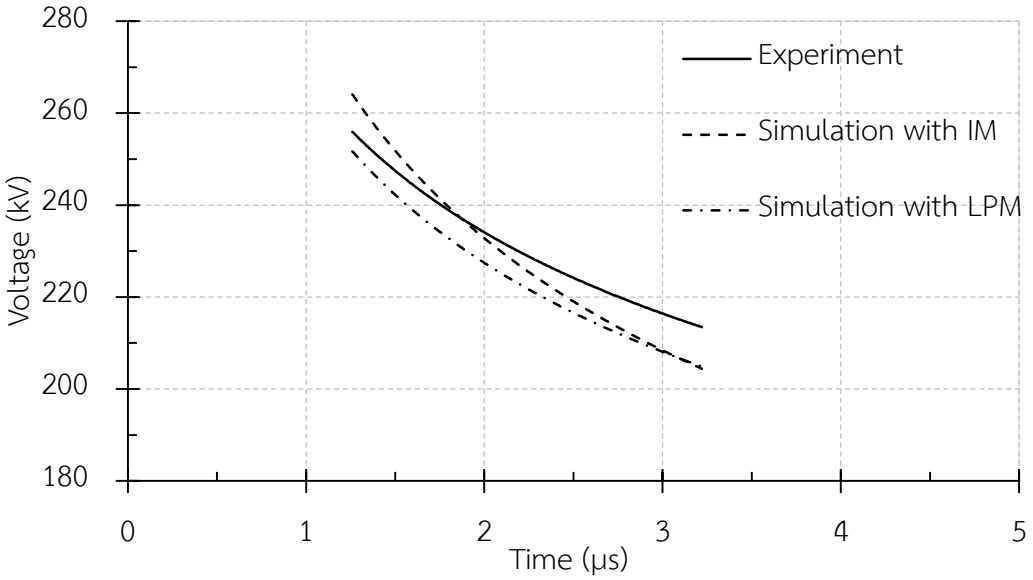

(*a*) Positive polarity

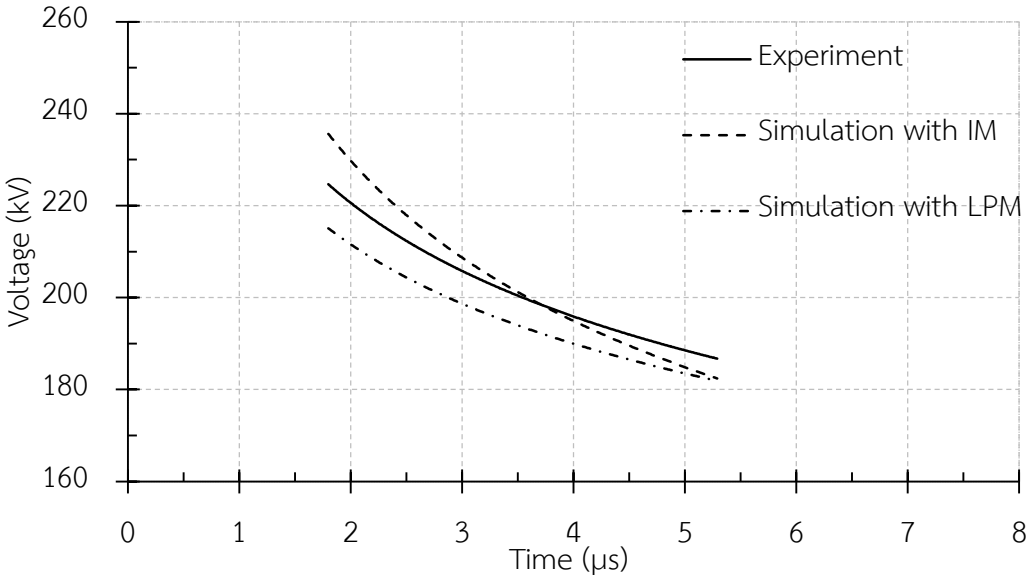

(*b*) Negative polarity

Figure 5.2 The comparison between volt-time characteristics which obtained from experiment and simulation of 2-disc ANSI class 52-1 insulator string under standard lightning impulse voltages of (*a*) Positive polarity and (*b*) Negative polarity

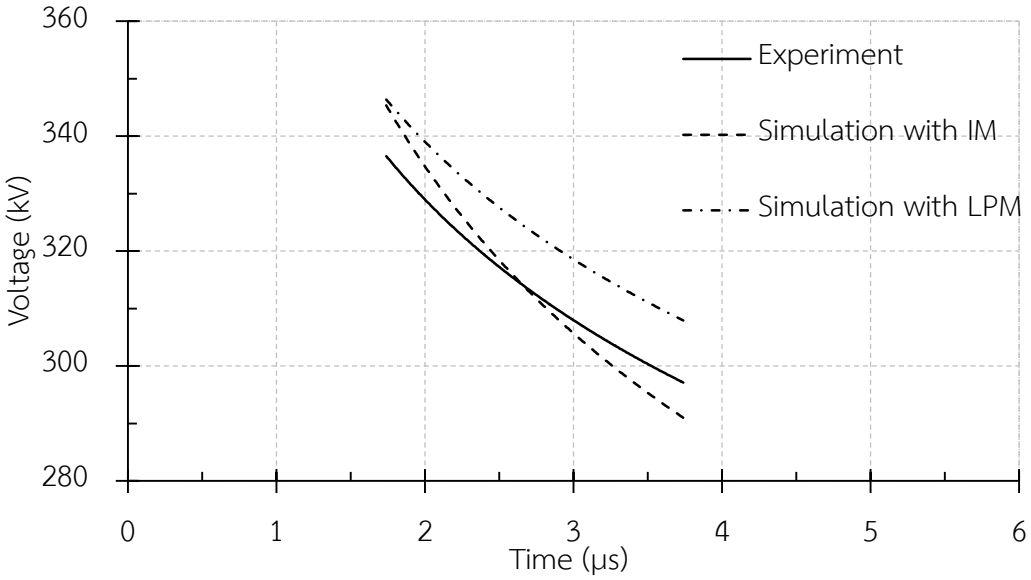

(*a*) Positive polarity

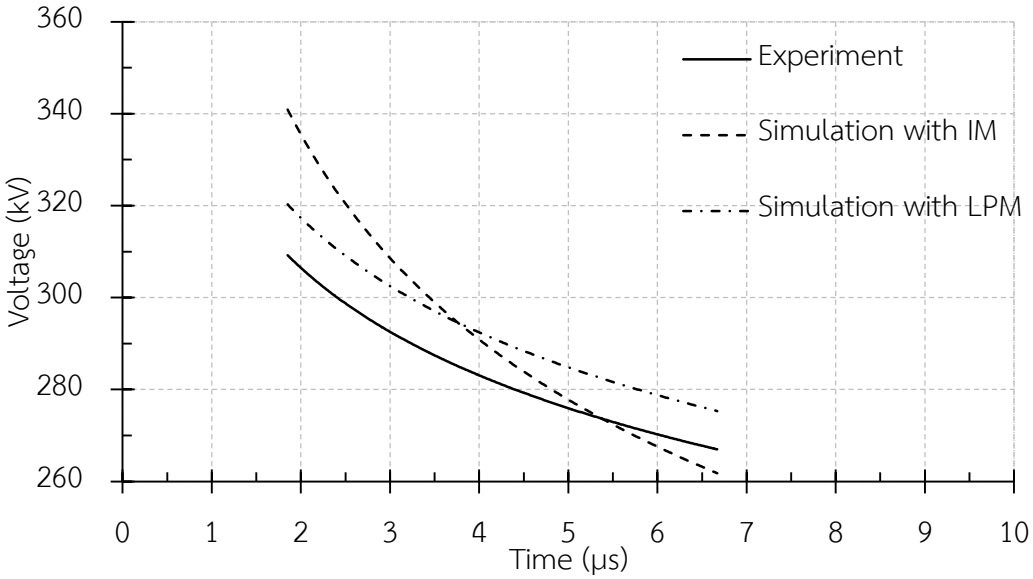

(*b*) Negative polarity

Figure 5.3 The comparison between volt-time characteristics which obtained from experiment and simulation of 3-disc ANSI class 52-1 insulator string under standard lightning impulse voltages of (*a*) Positive polarity and (*b*) Negative polarity

5.1.1.2 ANSI class 52-2 insulators string

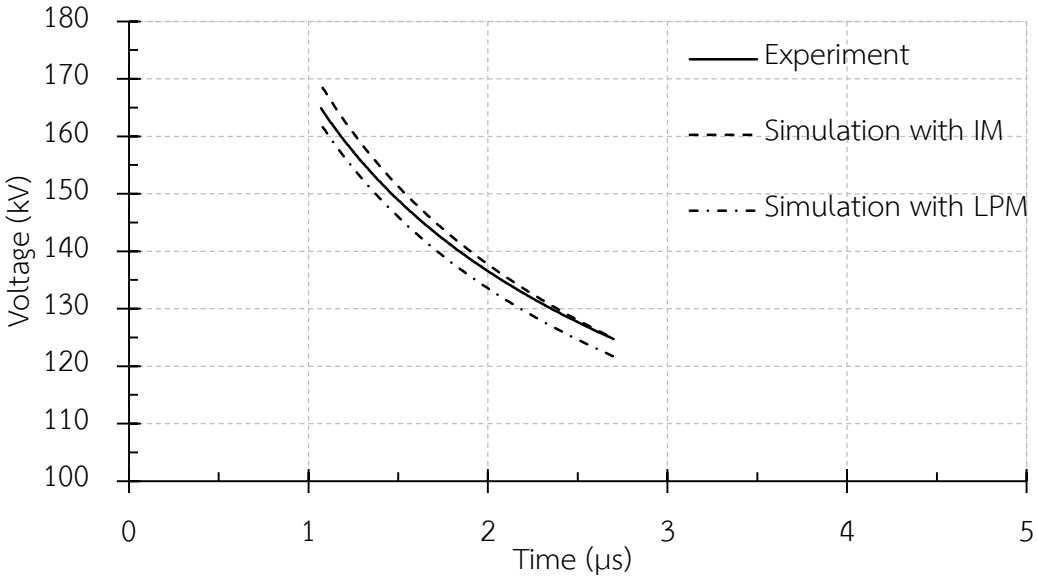

(*a*) Positive polarity

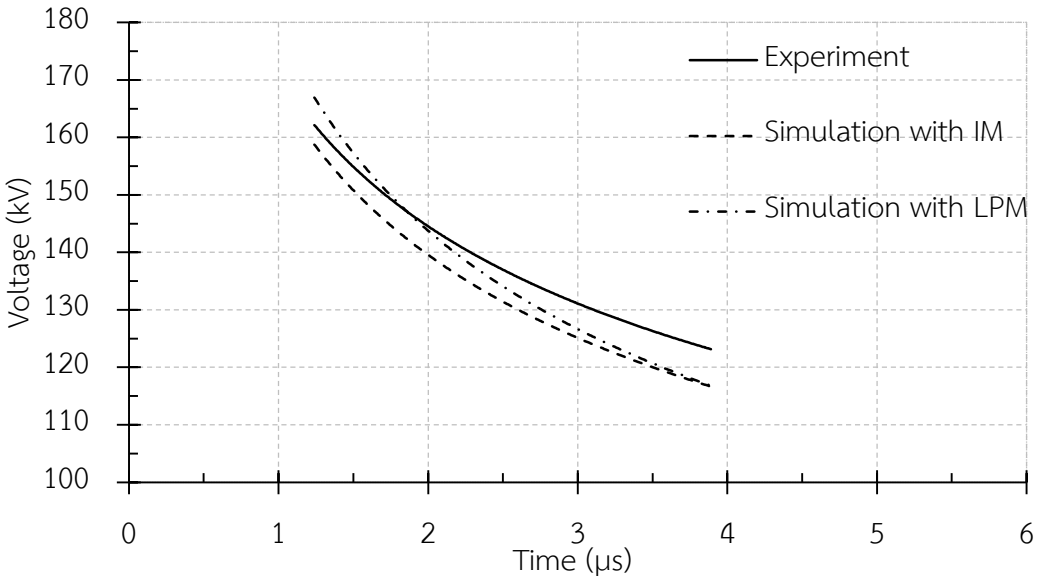

(*b*) Negative polarity

Figure 5.4 The comparison between volt-time characteristics which obtained from experiment and simulation of 1-disc ANSI class 52-2 insulator under standard lightning impulse voltages of (*a*) Positive polarity and (*b*) Negative polarity

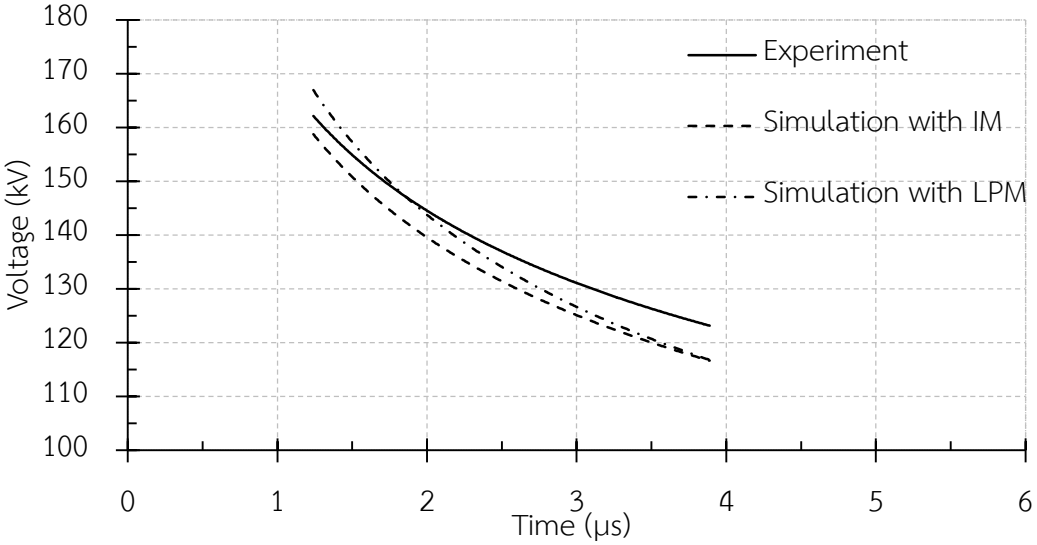

(*a*) Positive polarity

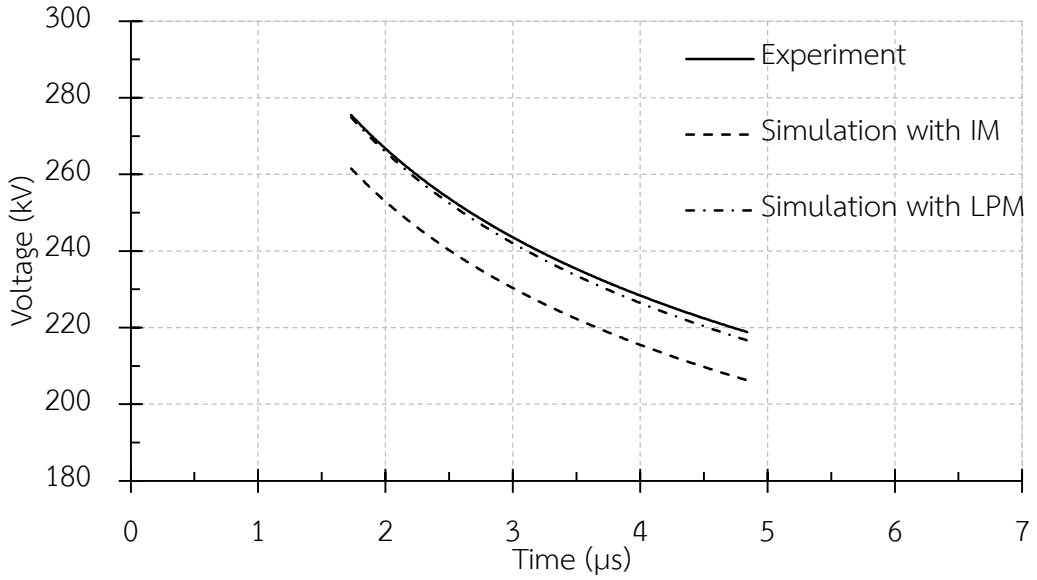

(*b*) Negative polarity

Figure 5.5 The comparison between volt-time characteristics which obtained from experiment and simulation of 2-disc ANSI class 52-2 insulator string under standard lightning impulse voltages of (*a*) Positive polarity and (*b*) Negative polarity

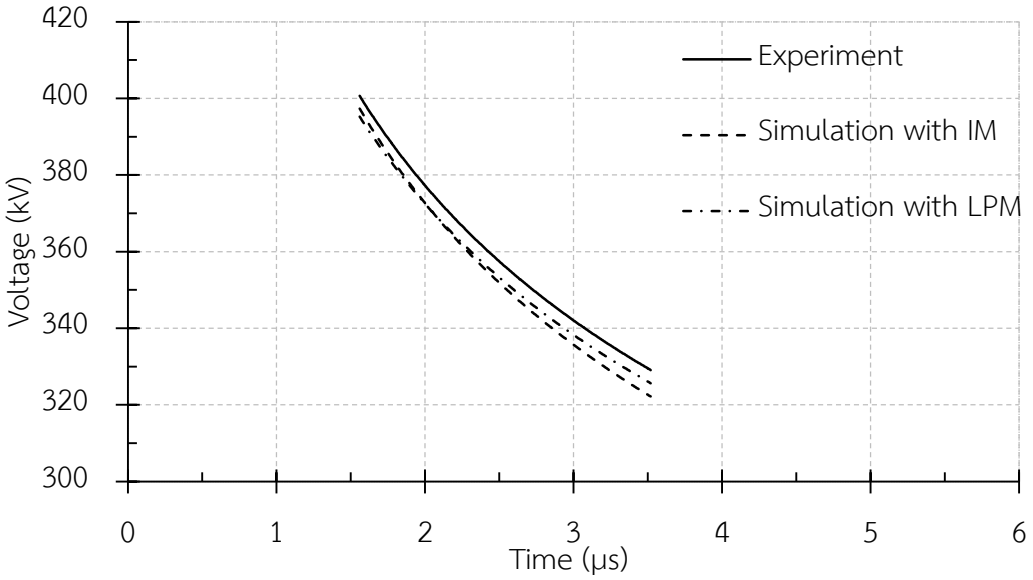

(*a*) Positive polarity

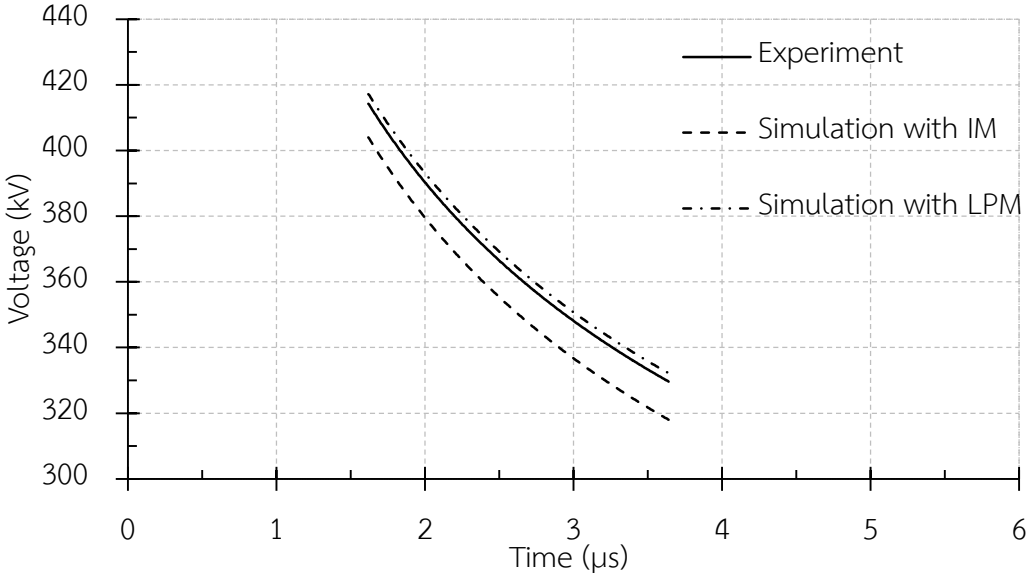

(*b*) Negative polarity

Figure 5.6 The comparison between volt-time characteristics which obtained from experiment and simulation of 3-disc ANSI class 52-2 insulator string under standard lightning impulse voltages of (*a*) Positive polarity and (*b*) Negative polarity

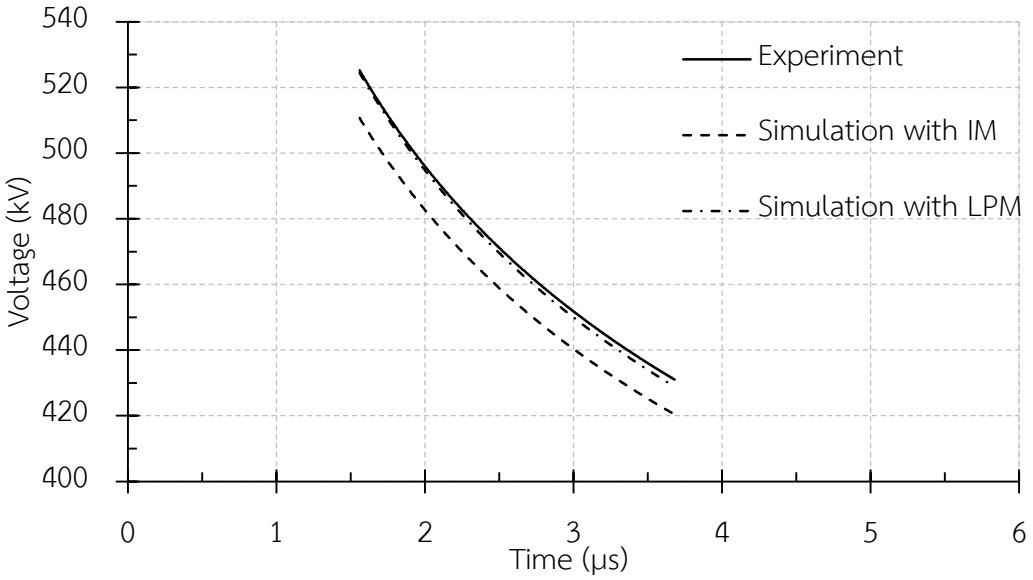

(*a*) Positive polarity

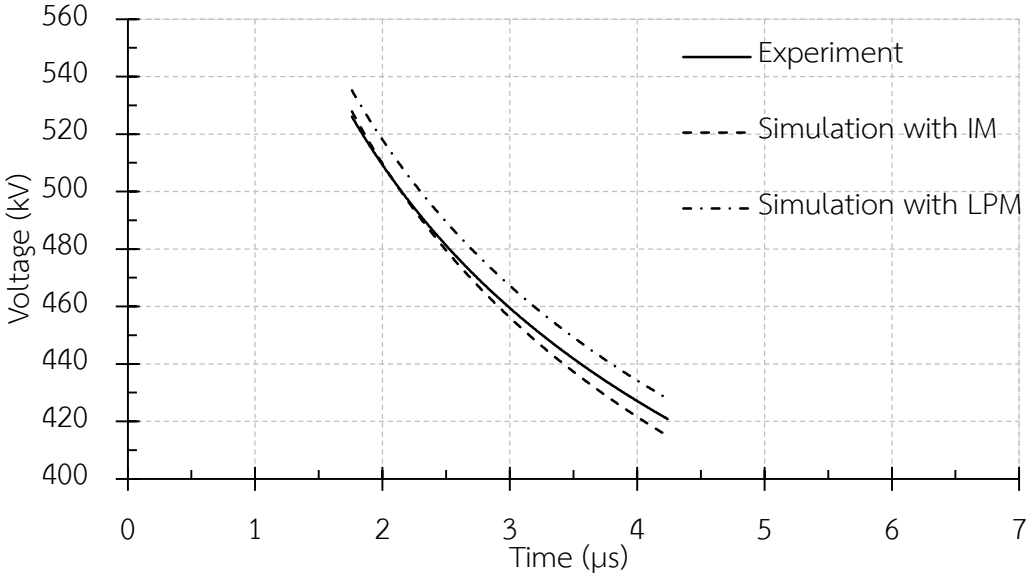

(*b*) Negative polarity

Figure 5.7 The comparison between volt-time characteristics which obtained from experiment and simulation of 4-disc ANSI class 52-2 insulator string under standard lightning impulse voltages of (*a*) Positive polarity and (*b*) Negative polarity

5.1.1.3 ANSI class 52-4 insulators string

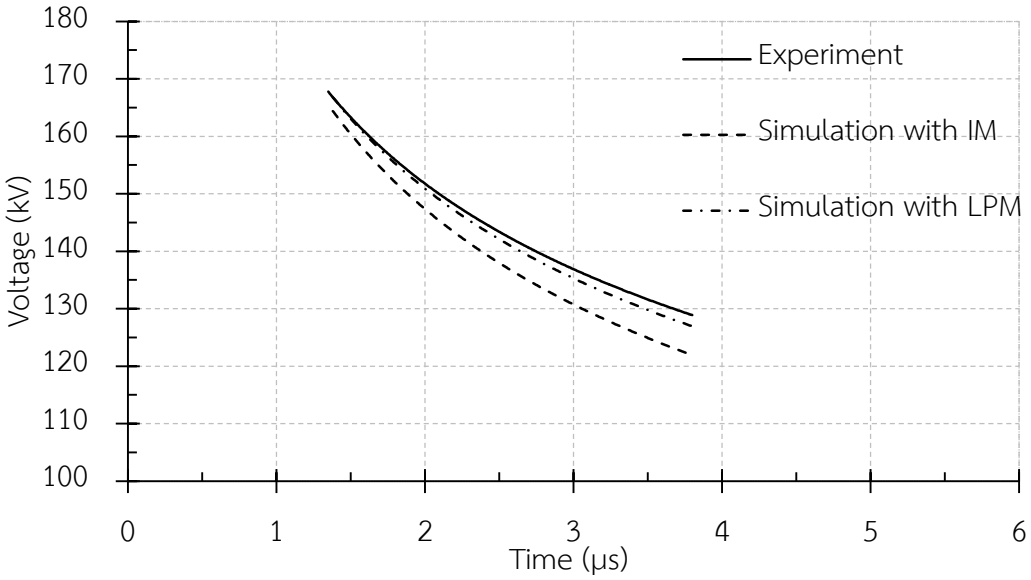

(*a*) Positive polarity

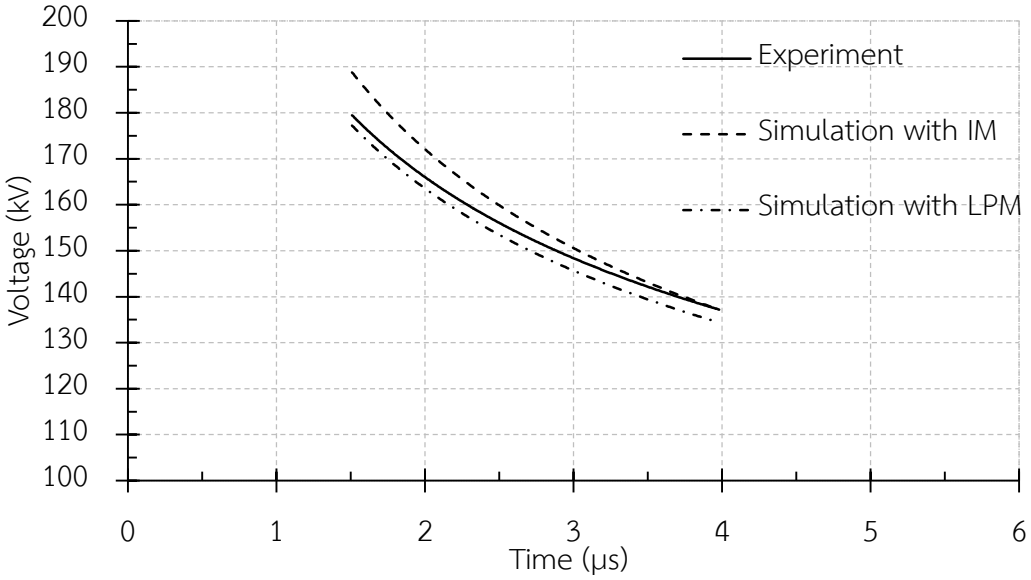

(*b*) Negative polarity

Figure 5.8 The comparison between volt-time characteristics which obtained from experiment and simulation of 1-disc ANSI class 52-4 insulator under standard lightning impulse voltages (*a*) Positive polarity and (*b*) Negative polarity

5.1.2. Case of non-standard lightning impulse (4.8/54.8 μs)

The case of non-standard, the IM cannot simulate, because the data of CFO for this case don't have. Then, this case will compare between the volt-time characteristics which obtained from experiment and simulation with LPM

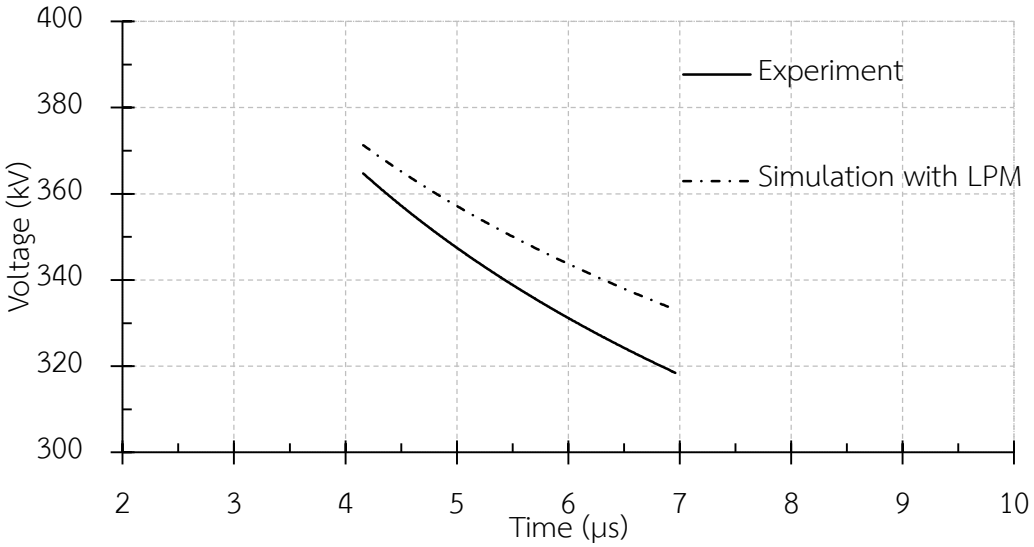

(*a*) Positive polarity

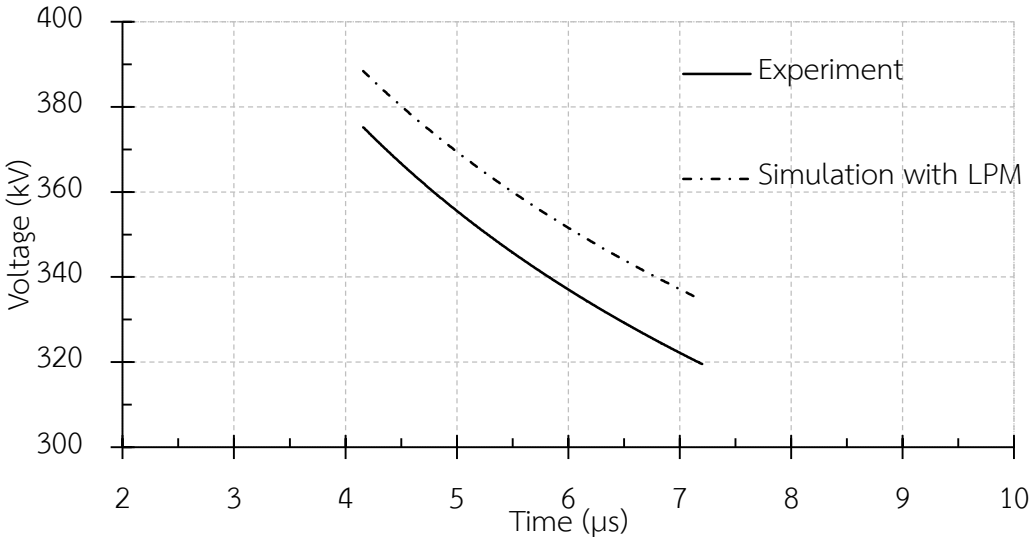

(*b*) Negative polarity

Figure 5.9 The comparison between volt-time characteristics which obtained from experiment and simulation of 3-disc ANSI class 52-2 insulator string under non-standard lightning impulse voltages of (*a*) Positive polarity and (*b*) Negative polarity

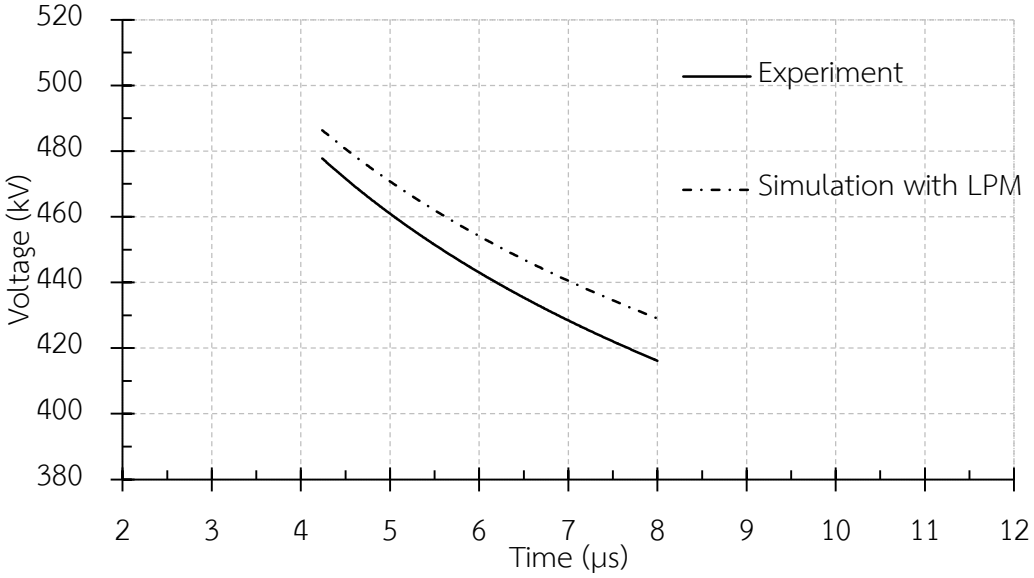

(*a*) Positive polarity

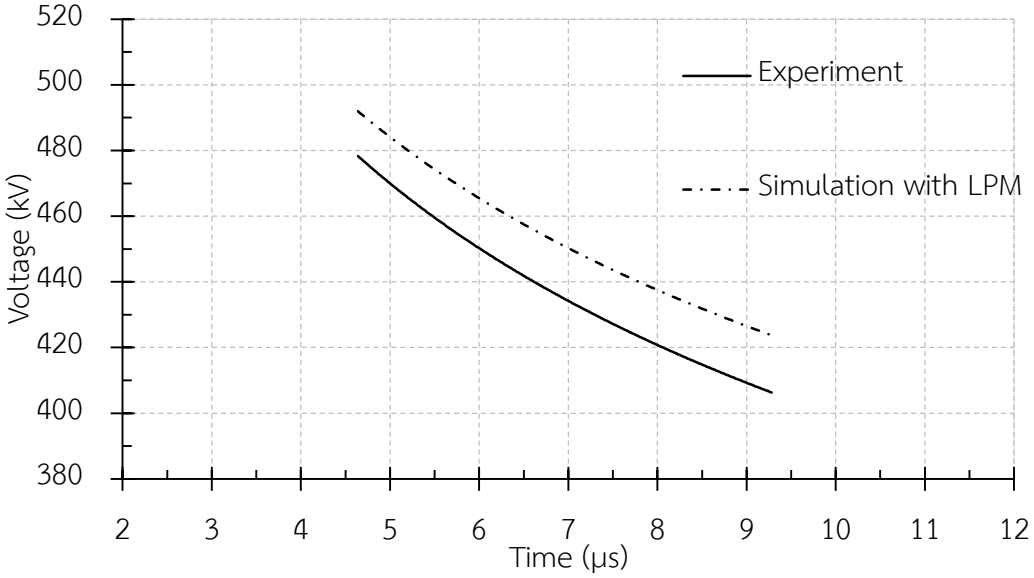

(*b*) Negative polarity

Figure 5.10 The comparison between volt-time characteristics which obtained from experiment and simulation of 4-disc ANSI class 52-2 insulator string under non-standard lightning impulse voltages of (*a*) Positive polarity and (*b*) Negative polarity

5.2. Calculation of the percent errors

From the figure 5.1 – the figure 5.10 which illustrate the comparison between the volt-time characteristics from the IM & LPM model and the experimental results. Both are almost approximate in the case of standard lightning impulse with both polarities and the case of non-standard lightning impulse voltages with both polarities. However, they still has a little bit of error because in the practice is different with the theory. In fact, the testing in laboratory is statistical e.g. determining the time lags, by applying in the same voltage level, but it often provide differently values of time lags, so determining a time lag is statistical, it also depend on the atmospheric i.e. pressure, temperature, humidity etc., the apparatus i.e. impulse generator, measurement systems etc. But the model in software computer use the mathematic equation, it calculate exactly e.g. determining a chopping time, by input the voltage in the model, it always provide the same value, so the model depend on the input data.

To calculate the percent errors of the comparison between both volt-time characteristics as mentioned earlier. Each point of chopping time from experimental results are the main values. By changing the magnitude of impulse voltage in the model until got the same value of the chopping time with the experimental results of each point. Then, the breakdown voltages of each point of both are used to calculate the percent errors and determine the maximum percent error of each point to analyze in this thesis.

Therefore, the percent errors calculated by equation below

$$\%_{Error} = \left| \frac{\#_{Experimental} - \#_{Simulation}}{\#_{Experimental}} \right| \times 100\% \qquad (5.1)$$

Where:

$\#_{Experimental}$ - Experimental value

$\#_{Simulation}$ - Simulation value

Hence, the results which calculated from equation above of the maximum errors of each volt-time characteristics of each type insulator string which was applied

or simulated by standard lightning impulse voltages and non-standard lightning impulse voltage of both polarities are shown in the table 5-1 and the table 5-2.

Table 5-1 The maximum percent errors for standard lightning impulse

Insulator	Polarity	No. of discs	Maximum (IM) %Errors (%)	Maximum (LPM) %Errors (%)
52-1	Positive	1	4.35	7.52
		2	4.21	3.98
		3	2.70	3.60
	Negative	1	18.98	11.63
		2	5.15	4.12
		3	10.38	3.77
52-2	Positive	1	3.07	2.54
		2	0.72	2.44
		3	2.08	1.41
		4	6.80	1.21
	Negative	1	5.86	4.65
		2	5.87	1.08
		3	3.69	0.90
		4	1.41	2.04
52-4	Positive	1	4.96	1.15
	Negative	1	7.28	2.44

Form the table 5-1, it can be seen that the LPM model can give more accurate results than the IM model in many cases.

Table 5-2 The maximum percent errors for non-standard lightning impulse

Insulator	Polarity	No. of discs	Maximum (LPM) %Errors (%)
52-2	Positive	3	4.01
		4	3.49
	Negative	3	4.69
		4	4.03

5.3. Determine critical flashover voltages (CFO)

Beside the simulation of breakdown for establishing the volt-time characteristics, the leader progression model can also be applied to determine the critical flashover voltages (CFO). CFO is the crest value of standard lightning impulse voltages for which the insulation result in a 50% probability of flashover or withstand. Another name of the CFO is called as $V_{50\%}$. It is widely used in the insulation co-ordination studies to describe the lightning impulse strength of high voltage insulators. The probability distribution of breakdown is show in figure 5.11.

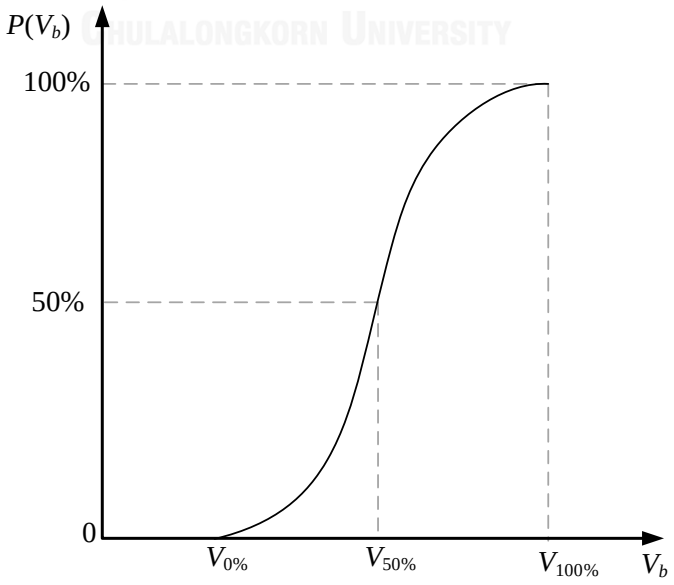

Figure 5.11 Breakdown probability distribution

Additional, the critical Flashover voltage (CFO), in view of physics, is defined as the minimum voltage above which all the electrons in the enclosed gap acquire enough energy to change the dielectric become to the conductive. Gaussian distribution is characterized by mean and standard deviation (σ). Mean value of 50 % value is termed Critical Flashover Voltage.

In general, the values of $V_{0\%}$ and $V_{100\%}$ are determined by using the value of $V_{50\%}$ and its standard deviation (σ) as following equation

$$V_{0\%} = V_{50\%} - 3\sigma \tag{5.2}$$

$$V_{100\%} = V_{50\%} + 3\sigma \tag{5.3}$$

CFO is equal to the asymptotic value of the volt-time characteristics. For air insulation, CFO are proposed to occur at about a time to breakdown of 16 μs [5, 30]. The LPM is, therefore, used to determine the peaks of impulse voltages that can cause the flashover of insulator strings at a time around 16 μs. The obtained voltages are compared with the CFOs of insulator strings obtained from experiments in ref. [14] and ref. [15]. Ref [14] studied the CFOs of insulator strings with 1-4 discs. Ref. [15] studied the CFOs of insulators strings with 4-7 discs installed with rod-rod and sphere-sphere arcing horns. Gap length between arcing horns for each case is shown in table 5-3

Table 5-3 Gap lengths of ANSI 52-4 with arcing horn rod-rod gap and sphere-sphere gap ref [15].

Insulator	No. of discs	Gap lengths (mm)	
		Rod-rod	Sphere-sphere
52-4	4	419	394
	5	565	540
	6	711	686
	7	857	832

By the same calculation as dry arcing distance mentioned before, the gap lengths can be determined as a function of insulator height multiply with disc number as follows:

- For the insulator strings install with arcing horn rod-rod gap:

$$d = n \times H - 164 \tag{5.4}$$

- For the insulator strings install with arcing horn sphere-sphere gap:

$$d = n \times H - 190 \tag{5.5}$$

By the same method with the simulation of volt-time characteristics mentioned before, the constant values of K and E_0 can be proposed as show in the table 5-4

Table 5-4 The constant values K and E_0 for ANSI Class 52-4 insulator string with arcing horns

Insulators	Polarity	$K\left(\frac{\mathrm{m}^2}{\mathrm{kV}^2\mathrm{sec}}\right)$	$E_0\left(\frac{\mathrm{kV}}{\mathrm{m}}\right)$
52-4 (rod-rod)	Positive	0.9	640
	Negative	0.9	640
52-4 (sphere-sphere)	Positive	3	677
	Negative	3	677

The results of simulated CFOs obtained from the LPM and their percent errors in comparison with experimental ones are shown in the table 5-5 and the table 5-6

Table 5-5 The percent errors for CFOs of 1-4 disc insulator strings without arcing horns

Insulator	Polarity	No. of discs	$V_{50\%}$ or CFO (kV)		%Errors (%)
			Experiment	Simulation	
52-1	Positive	1	103.62	98.00	5.42
		2	202.48	203.10	0.31
		3	292.13	308.00	5.43
	Negative	1	98.41	88.90	9.66
		2	182.42	184.50	1.14
		3	265.45	280.00	5.48
52-2	Positive	1	121.32	114.10	5.95
		2	215.21	216.80	0.74
		3	318.11	319.59	0.47
		4	419.367	422.30	0.70
	Negative	1	119.74	113.00	5.63
		2	207.47	214.70	3.48
		3	308.92	316.40	2.42
		4	405.53	418.20	3.12
52-4	Positive	1	121.65	125.5	3.16
	Negative	1	130.92	130.35	0.44

Table 5-6 The percent errors for CFOs of 4-7 disc insulator strings with arcing horns

Insulator	Polarity	No. of discs	$V_{50\%}$ or CFO (kV)		%Errors (%)
			Experiment	Simulation	
52-4 (rod-rod)	Positive	4	287	276.1	3.80
		5	386	372.2	3.58
		6	462	468	1.30
		7	550	564	2.55
	Negative	4	287	276.1	3.80
		5	386	372.2	3.58
		6	462	468	1.30
		7	557	564	1.26
52-2 (sphere-sphere)	Positive	4	284	269	5.28
		5	381	368	3.41
		6	447	466	4.25
		7	551	565.8	2.69
	Negative	4	283	269	4.95
		5	387	368	4.91
		6	461	466	1.08
		7	559	565.8	1.22

It can be seen that the proposed model based on LPM can estimate the values of CFO with an error less than 6%.

CHAPTER 6

CONCLUSIONS AND SUGGESTIONS

6.1. Conclusions

This thesis studied the application of integration model (IM) and leader progression model (LPM) to simulate the flashover of suspension insulator strings. The values of parameters for both models are proposed to simulate and establish the volt-time characteristics of suspension insulator strings under 1.2/50 μs standard impulse voltage and 4.8/54.8 μs non-standard impulse voltage of both positive and negative polarities. To verify the proposed models, the simulation results are compared with the experimental ones. Test objects are insulator strings with 1-4 discs of ANSI class 52-1, 1-4 discs of ANSI class 5-2 and 1 disc of ANSI class 52-4. The proposed model based on LPM is also applied to determine the critical flashover voltage (CFO) of insulator strings. The estimated results are compared with the experimental ones. All obtained results can be concluded as follows:

1. For simple IM, when the impulse voltage applied across an insulator string exceeds a threshold level *Vo*, the energy required to complete the breakdown process is constant which is called disruptive effect *DE*. The values of *Vo* are proposed to be 90% of CFO while the value of *DE* are proposed as a function of dry arcing distance of insulator string for impulse voltage of each polarity. It is found that the model based on such simple integration method can predict voltage-time characteristics of insulator strings with larger errors when compared with that based on leader progression method.

2. The LPM is based on the physical breakdown process. When the gradient generated by the impulse exceeds a threshold level *Eo*, a differential equation must be solved to determine leader progression speed and leader length until it reaches the dry arcing distance. The values of three parameters are proposed for the model based on LPM, i.e. critical gradient *Eo*, leader coefficient *K* and dry arcing distance *d*.

However, *d* can be estimated if disc height and number of discs are known. With the values of parameters proposed in this thesis, the errors in predicting the voltage-time characteristics of insulator strings are found to be less than 5% for insulator strings with 2-4 discs under standard and non-standard impulse voltages with both polarities.

3. The proposed model based on LPM can also be applied to predict the CFOs of insulator strings. The predicted CFOs of 1-4 disc insulator strings without arcing horn and 4-7 disc insulator string with arcing horns show a good agreement with the experimental results. The deviations are within 6% except one case that reaches 10%.

6.2. Suggestions

1. Further study shall be performed to verify the capability of the proposed model to predict the voltage-time characteristics of insulator strings under impulse voltage with fast front time.

2. Further study shall be performed to verify the capability of the proposed model to predict the CFOs of insulator strings under non-standard impulse voltage.

3. More understanding in the breakdown process of insulator strings is important for the development of more accurate simulation model.

REFERENCES

[1] IEC 60071-1, "Insulation Co-ordination – Part 1: Definitions, principles and rules," Edition 8.0, 2006.

[2] IEC 60071-2, "Insulation Co-ordination – Part 2: Application Guide," Edition 3.0, 1996.

[3] CIGRE WG 33-01, "Guide to procedures for estimating the lightning performance of transmission lines," *Technical Bulletin 63*, Oct. 1991.

[4] Report Prepared by the Fast Front Transients Task Force of the IEEE Modeling and Analysis of System Transients Working Group, "MODELING GUIDELINES FOR FAST FRONT TRANSIENTS," in IEEE Transactions on Power Delivery, Vol. 11, No. 1, January 1996.

[5] Dalibor Filipović-Grčić, Božidar Filipović-Grčić, Danijel Brezak, Ivo Uglešić, and Amir Tokić, "Leader Progression Model Application for Calculation of Lightning Critical Flashover Voltage of Overhead Transmission Line Insulators," in International Conference on Lightning Protection (ICLP), Vienna, Austria, 2012.

[6] Zacharias G. Datsios, Pantelis N. Mikropoulos, and Thomas E. Tsovilis, "Insulator String Flashover Modeling with the aid of an ATPDraw Object," in UPEC 2011 46th International Universities' Power Engineering Conference, Soest, Germany, 5-8th September 2011.

[7] Takatoshi Shindo, and Toshio Suzuki, "A NEW CALCULATION METHOD OF BREAKDOWN VOLTAGE-TIME CHARACTERISTICS OF LONG AIR GAPS," in IEEE Transactions on Power Apparatus and Systems, Vol. PAS-104, No. 6, June 1985.

[8] P. Chowdhuri, A. K. Mishra, and B. W. McConnell, "Volt-Time Characteristics of Short Air Gaps Under Nonstandard lightning Voltage Waves," in IEEE Trans. On Power Delivery, Vol.12, no.1, 1997.

[9] M. Darvenizia, and A. E. Vlastos, "The Generalized Integration Method for Predicting Impulse Volt-Time Characteristics for non-Standard Wave Shapes a Theoretical Basis," in IEEE fiansactions on Electrical Insulation, 1988.

[10] S. Sekioka, and et al., “Calculation of Flashover Characteristics in the EMTP,” in Trans. On IEE Japan, Japan, 1993.

[11] *ATP/EMTP Rule Book*: Canadian-American EMTP Users Group.

[12] H. W. Dommel, *EMTP THEORY BOOK*, Vancouver, British Columbia: Microtran Power System Analysis Corporation, 1996.

[13] L. Prikler, and H. K. Høidalen, *ATPDRAW version 5.6 Users' Manual*: Preliminary Release No. 1.0, November, 2009.

[14] K. Othanu, and N. Tanthanuch, “Voltage-time Characteristics on Suspension Insulator in 24 kV Distribution System,” in PW037, EECON-36, 2013.

[15] R. Witthawat, “INFLUENCE OF IMPLUSE WAVE FRONT ON FLASHOVER VOLTAGE OF SUSPENSION INSULATOR STRINGS,” Electrical Engineering, Chulalongkorn University, Bangkok, Thailand, 2009.

[16] IEC 60060-1, "High-voltage test technique – Part 1: General definitions and test requirements," Edition 3.0, 2010.

[17] D. Kind, *An Introduction to High-Voltage Experimental Technique*, Germany: W. Langelüddecke, Braunchweig, 1978.

[18] J. M. Meek, and J. D. Craggs, *ELECTRICAL BREAKDOWN OF GASES*, London: Oxford University Press, Amen House, 1953.

[19] J. Townsend, *Electricity in Gases*: Clarendon Press, 1915.

[20] M. S. Naidu, and V. Kamaraju, *High Voltage Engineering*, Second ed., New Delhi: Tata McGraw-Hill Publishing Company Limited, 2002.

[21] E. Kuffel, W. Zaengl, and J. Kuffel, *HighVoltage Engineering Fundamentals*, Second ed., Oxford: Butterworth-Heinemann, 2000.

[22] D. V. Razevig, *HIGH VOLTAGE ENGINEERING*, 2-B, Nath Market, Delhi-110006: Khanna Plublishers, 1985.

[23] J. R. Lucus, *High Voltage Engineering*, Srilanka: University of Moratuwa, 2001.

[24] สำรวย สังข์สะอาด, วิศวกรรมไฟฟ้าแรงสูง, Bangkok: Electrical department, Faculty of Engineering, Chulatongkorn University, March,2006.

[25] M. Abdel-Salam, H. Anis, A. El-Morshedy, and R. Radwan, *High-Voltage Engineering*, Sencond ed., New York: Marcel Dekker, Inc, 2000.

[26] J. S. T. Looms, *Insulators for HIGH VOLTAGES*, London, United Kingdom: Perter Peregrinus, 1988.

[27] U. A. Bakshi, and M. V. Bakshi, *Electrical Power Transmission & Distribution*, Pune: Techical Publications Pune, 2007.

[28] K. Wanit, " A STUDY ON LIGTHNING IMPULSE BREAKDOWN CHARACTERISTICS OF ARCING HORNS FOR POWER TRANSFORMER PROTECTION," Electrical Engineering, Chulalongkorn University, Bangkok, Thailand, 2010.

[29] R. O. Calwell, and M. Darveniza, "Experimental and Analytical Studies of the Effect of Non-Standard Wave Shapes on the Impulse Strength of External Insulation," *IEEE Trans., Pwr App. and Syst.,* vol. 92, pp. 1420-1428, 1973.

[30] A.R. Hileman, *Insulation Coordination for Power Systems*, New York: Marcel Dekker, Inc, 1999.

APPENDIX

VITA

Khamphasith Inthoulath was born in Vientiane, Lao PDR., in 1988. He received the Bachelor's degree of Electrical Engineering from Faculty of Engineering, National University of Laos in 2010. In June, 2012, he studied master's degree at Electrical Engineering Department, Faculty of Engineering, Chulalongkorn University.